

Illustrated Brazilian consensus of terms and fundamental patterns in chest CT scans*

Consenso brasileiro ilustrado sobre a terminologia dos descritores e padrões fundamentais da TC de tórax

C. Isabela S. Silva, Edson Marchiori, Arthur Soares Souza Júnior, Nestor L. Müller, Comissão de Imagem da Sociedade Brasileira de Pneumologia e Tisiologia

Abstract

The objective of this new Brazilian consensus is to update and to continue the standardization of the principal terms and fundamental patterns in chest CT scans in Portuguese. There is a succinct definition of the principal terms used to describe chest CT findings, as well as illustrations of classic examples. The group of authors comprised radiologists specializing in chest radiology and holding membership in the Brazilian College of Radiology and Diagnostic Imaging, as well as pulmonologists having a special interest in diagnostic imaging and holding membership in the Brazilian Thoracic Association.

Keywords: Lung; Consensus; Tomography.

Resumo

O objetivo deste novo consenso brasileiro é atualizar e dar continuidade à padronização da terminologia dos principais descritores e padrões fundamentais da TC de tórax em língua portuguesa. Este consenso contém uma descrição sucinta dos principais termos utilizados na TC de tórax e ilustrações de exemplos clássicos. O grupo de autores é formado por médicos radiologistas membros do Colégio Brasileiro de Radiologia e Diagnóstico por Imagem, especializados em radiologia torácica, e por pneumologistas membros da Sociedade Brasileira de Pneumologia e Tisiologia, com particular interesse em diagnóstico por imagem.

Descritores: Pulmão; Consenso; Tomografia.

Introduction

In the evaluation of patients with thoracic diseases, CT scans are a diagnostic tool of great importance. In recent years, new CT patterns have been recognized, new terms have been coined in order to describe CT findings in English, and some terms have become obsolete.⁽¹⁻⁴⁾ Despite the great dissemination of the Brazilian Consensuses published in 2002 and in 2005, respectively, in the journal *Radiologia Brasileira* (Brazilian Radiology), the official organ of the Brazilian College of Radiology and Diagnostic Imaging, and in the Brazilian Journal of Pulmonology, the official organ of the Brazilian Thoracic Association, some terms have yet to be stand-

ardized in Portuguese.^(5,6) The publication of the new Fleischner Society Glossary of Terms, in 2008,⁽⁷⁾ motivated a group of radiologists and pulmonologists (members of the Brazilian College of Radiology and Diagnostic Imaging who specialize in chest radiology and members of the Brazilian Thoracic Association who have a special interest in diagnostic imaging) to develop a new version of the Brazilian Consensus. The principal objective of this update is to continue the standardization of the principal terms used, in an easy-to-read and succinct way, as well as to illustrate the principal terms and patterns in chest CT scans using classic examples.

* Study carried out by the *Sociedade Brasileira de Pneumologia e Tisiologia* – SBPT, Brazilian Thoracic Association – Brasília, Brazil. Correspondence to: C. Isabela S. Silva. Department of Radiology, University of British Columbia/Vancouver General Hospital, 3350-950 West 10th Avenue, Vancouver, BC V5Z 4E3, Canada.

Tel 1 604 875-4165. Fax 1 604 875-4319. E-mail: c.isabela.silva@gmail.com

Financial support: None.

Submitted: 15 July 2009. Accepted, after review: 17 July 2009.

Note to readers: The original document was composed in Portuguese, and this (translated) glossary of terms in English is therefore alphabetized by the names of the corresponding terms in Portuguese.

Glossary¹

Air trapping (aprisionamento aéreo)

Air trapping is the retention of excess gas (air) in part of or all of the lung (especially upon exhalation), resulting from partial or total airway obstruction or secondary to focal abnormalities of lung compliance. It is recognized during the expiratory phase as reduced attenuation of the lung parenchyma, especially apparent as lower-than-usual density (Figure 1) and absence of volume reduction.⁽⁶⁻¹⁰⁾

See also Mosaic attenuation/perfusion pattern.

Atelectasis (atelectasia)

Atelectasis is the reduction in lung volume caused by the reduced aeration of all or part of the lung.⁽¹¹⁾ It is observed as a combination of reduced attenuation of the lung parenchyma and reduction in lung volume, characterized by the displacement of fissures, of mediastinal structures or of the diaphragm and by the approximation of the bronchovascular struc-

tures of the affected parenchyma (Figures 2 and 3).^(3,12) With regard to distribution, the following types of atelectasis can be found: subsegmental, segmental, lobar or whole lung. Atelectasis can also be qualified, according to its form, as plate-like (discoid) or rounded.⁽¹³⁾ In studies using iodinated contrast material, the homogeneous enhancement of the lung parenchyma can aid in the differentiation between atelectasis and consolidation (Figure 3). The term “collapse” can be used in cases of total atelectasis of one lobe or whole lung atelectasis.

Plate-like atelectasis (atelectasia laminar)

Plate-like atelectasis is a focal area of subsegmental atelectasis with linear or discoid configuration, almost always extending to the pleura (Figure 4). It is generally horizontal or oblique, but it can also have a vertical orientation. The thickness of laminar atelectasis can range from a few millimeters to over 1 cm.⁽¹⁴⁾ Laminar atelectasis is synonymous with discoid atelectasis.

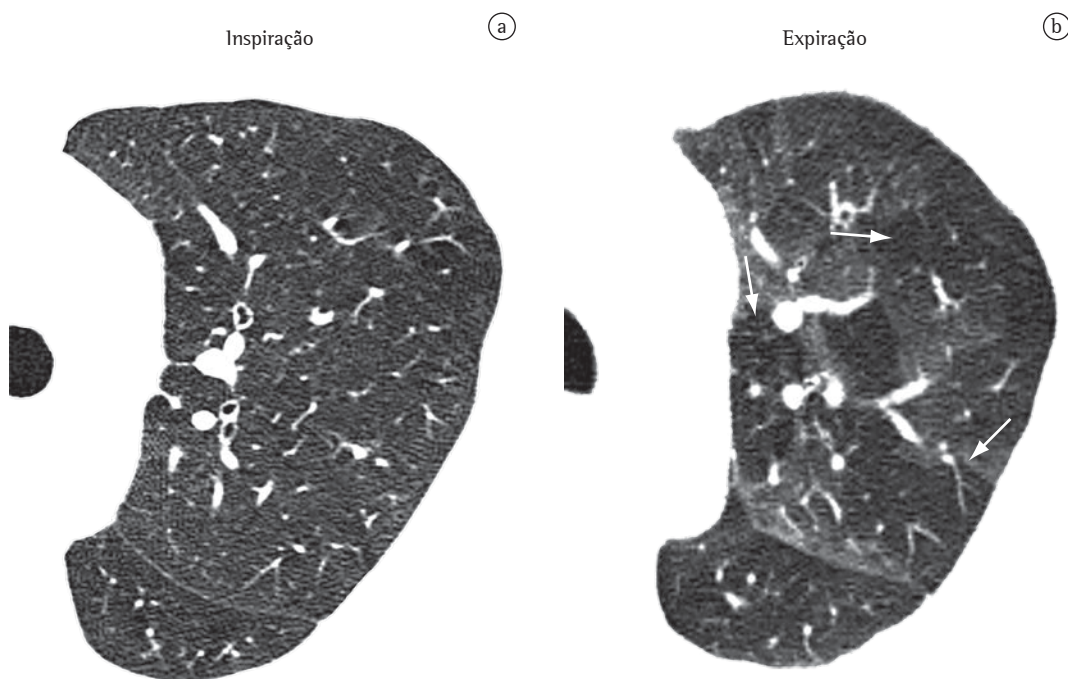


Figure 1 – Axial HRCT scan of the chest during inhalation (a), revealing no significant changes. HRCT scan of the chest during exhalation (b), revealing air trapping (arrows).

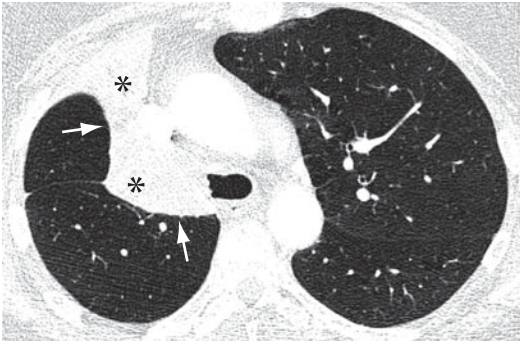


Figure 2 - Total atelectasis of the right upper lobe (asterisks) due to bronchial obstruction. Displacement of fissures (arrows) and ipsilateral deviation of the mediastinal structures are observed.

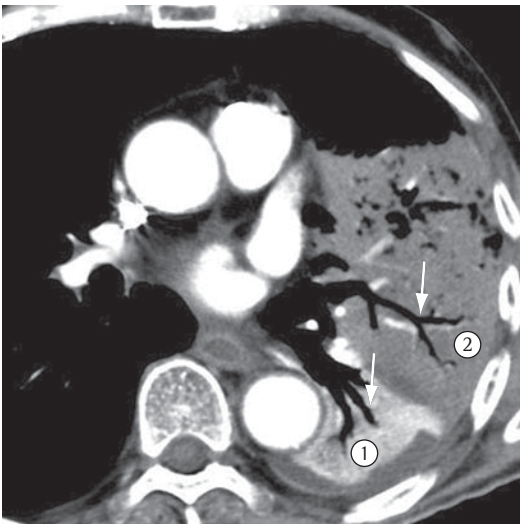


Figure 3 - Axial CT slice of the chest with iodinated contrast material, revealing air bronchograms (arrows) in areas of lung parenchyma with atelectasis (1) and consolidation (2). The segment of the lung parenchyma with atelectasis shows normal enhancement amid the iodinated contrast material (1).

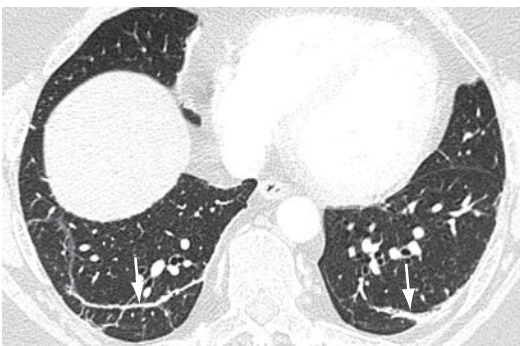


Figure 4 - Laminar atelectasis (arrows) on the lung bases.

Rounded atelectasis (atelectasia redonda)

Rounded atelectasis is a type of oval-shape atelectasis caused by the adherence of the adjacent lung parenchyma to the area of pleural thickening, for example, in cases of asbestos-related pleural disease or empyema resolution.⁽¹⁵⁾ It manifests as a rounded focal opacity to which bronchovascular structures converge (comet tail artifact) with a pleural base near the area of pleural thickening (Figure 5).^(16,17) It presents homogeneous enhancement when iodinated contrast material is used.

Parenchymal bands (banda parenquimatosa)

Parenchymal bands are linear opacities, generally peripheral and often in contact with the pleural surface, which might be thickened and retracted at the site of contact (Figure 6). They are usually 1-3 mm thick and at least 5 cm long.⁽⁹⁾ Parenchymal bands often have horizontal distribution (perpendicular to the pleural surface), but they can also have an oblique distribution. They generally indicate pleuroparenchymal fibrosis. Lung architecture distortions are often identified. Parenchymal bands are frequently found in patients exposed to asbestos.⁽¹⁸⁾

Fungus ball (bola fúngica)

A fungus ball results from the fungal colonization of preexisting pulmonary cavitation, generally secondary to tuberculosis or sarcoidosis, but it can also occur within cysts (e.g., bronchogenic cyst), bullae or dilated bronchi. Colonization by *Aspergillus* spp. is the most common type of colonization, and in this case, the term “aspergilloma” is used. A fungus ball is characterized by a mass-like collection of intertwined hyphae associated with mucus, fibrin, and cellular debris. On CT scans, a fungus ball is observed as a rounded or oval mass, which tends to hang down when images are acquired with the patient in different horizontal positions (Figure 7).⁽¹⁹⁾ Other common findings in this condition include the presence of the “air crescent sign”, amorphous calcification within the lesion, sponge-like appearance of the lesion and adjacent pleural thickening. The term “fungus ball” should not be used as a synonym

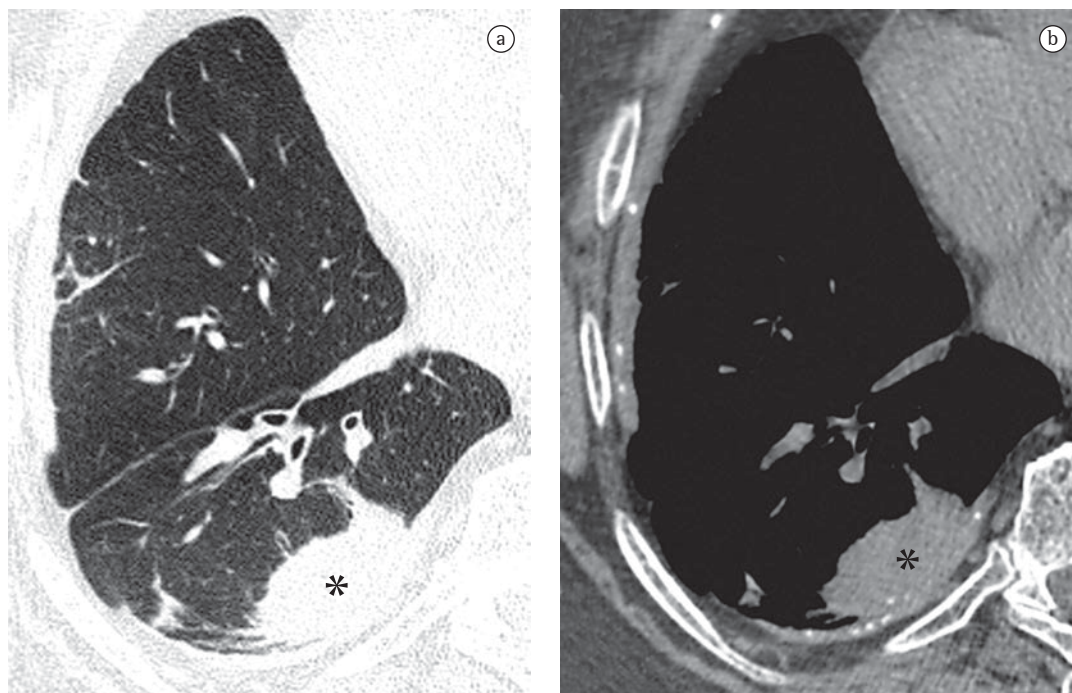


Figure 5 - Axial HRCT slices of the chest reconstructed with algorithms to evaluate the pulmonary parenchyma (a) and the mediastinum (b), revealing rounded atelectasis (asterisks) in a patient exposed to asbestos. Pleural thickening with calcification is also seen (b).

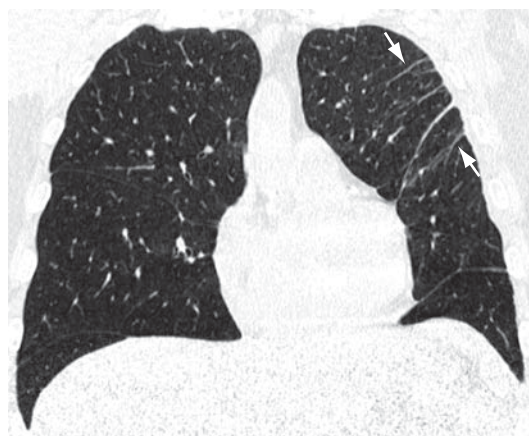


Figure 6 - Coronal reformatting of HRCT scan of the chest revealing parenchymal bands in the left upper lobe (arrows), with minimum irregularity on the adjacent pleural surface.

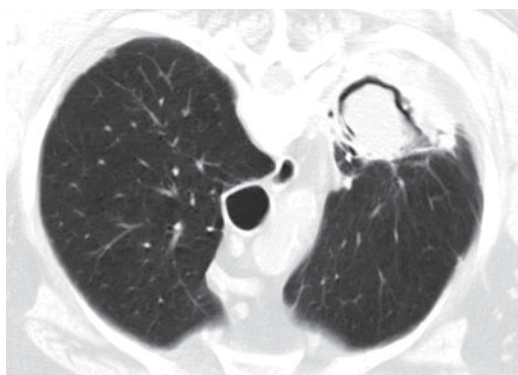


Figure 7 - Axial CT slice of the chest obtained with the patient in the prone position revealing a fungus ball with air crescent sign in residual tuberculous cavity. Associated pleural thickening is identified.

for “mycetoma”, since they represent different processes.⁽²⁰⁾

See also Air crescent sign and Mycetoma.

Bulla (bolha)

A bulla is a hypodense focal area that presents well-defined and smooth walls that do not exceed 1 mm in thickness (Figure 8).⁽⁴⁾ Bullae generally

have gaseous content, but they can also have an air-fluid level. In general, they are associated with other signs of pulmonary emphysema and have a paraseptal location (findings that aid in the differentiation from cysts on CT scans). They typically measure ≥ 1 cm in diameter. Bullae that are < 1 cm and located in the visceral pleura or in the subpleural region of the lung are known

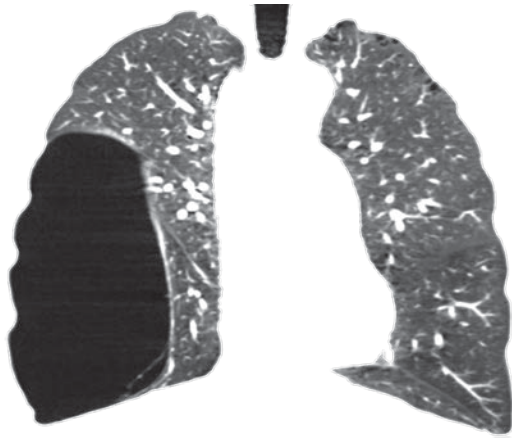


Figure 8 - Coronal reformatting of the HRCT of the chest revealing a large bullae in the right lower lobe and minimal centriacinar emphysema in the upper lobes.

as blebs in English.^(3,7) Blebs (tentatively translated to Portuguese as *vesículas*) that have an apical location are frequently responsible for primary spontaneous pneumothorax.

See also Bullous emphysema and Paraseptal, or distal acinar, emphysema.

Bronchocele (broncocele)

Bronchocele is characterized by bronchial dilation with secretion accumulation (mucoid impaction), generally caused by proximal obstruction, which might be congenital (e.g., bronchial atresia) or acquired (e.g., allergic bronchial aspergillosis).⁽²¹⁾ Bronchocele is observed as a tubular or branched image that resembles the finger of a glove (Figure 9). In cases of bronchial atresia, decreased attenuation of the lung parenchyma distal to the lesion can be observed on CT scans.

Air bronchogram (broncograma aéreo)

An air bronchogram is the radiological translation of air-filled bronchi, surrounded by sick lung parenchyma, in which the air of the airways has been substituted by any pathological material, radiologically denser than air (e.g., transudate, exudate, blood, accumulation product or neoplastic cells). In general, this is the expression used when a lucent (gas-filled) tubular region is seen within an area of opacified lung (Figures 3 and 10). This tubular image should be of a size and orientation typical of a

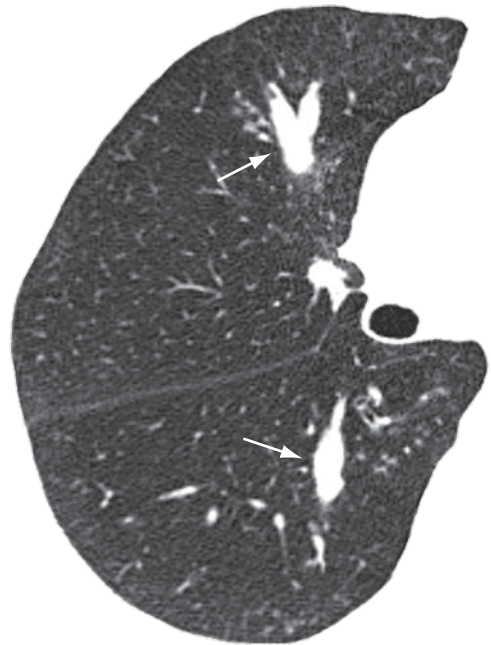


Figure 9 - Bronchocele (arrows).

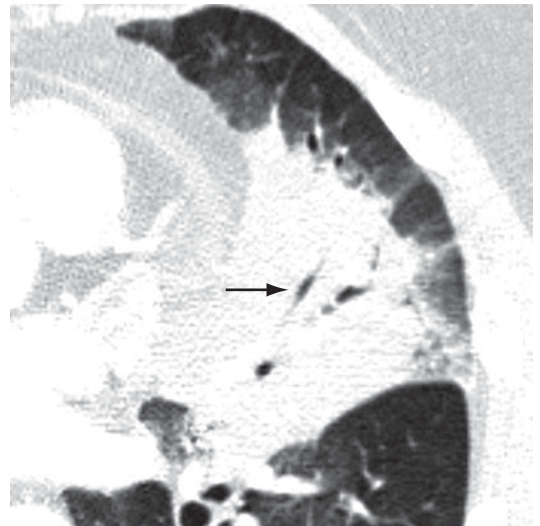


Figure 10 - Consolidation with air bronchograms (arrow).

bronchus or multiple bronchi, presumably representing a segment of the bronchial tree.^(22,23)

Broncholith (broncolito)

A broncholith is a calcified peribronchial lymph node that erodes into the adjacent bronchus. It is often secondary to infections by *Histoplasma* sp. or *Mycobacterium tuberculosis*. On CT scans, a broncholith is seen as a small

focus of calcification within or adjacent to the airway, being more common in the middle lobe bronchus (Figure 11). Mucoïd impaction, bronchiectasis or atelectasis might be observed distally.^(24,25)

Bronchiectasis (bronquiectasia)

Bronchiectasis is irreversible bronchial dilatation, which can be focal or diffuse. It generally results from chronic infection, proximal airway obstruction or congenital bronchial abnormalities. The morphological findings seen on HRCT scans (Figure 12) are as follows: the internal diameter of the bronchus is larger than the diameter of the adjacent pulmonary artery (signet-ring sign); loss of normal bronchial tapering, defined as the maintenance of the bronchial diameter for more than 2 cm, distally to the bifurcation (“tram tracks”); and identification of airway less than 1 cm from the pleural surface. Bronchiectasis is frequently associated with the thickening of the bronchial walls, mucoïd impaction and small airway changes.^(26,27) Pathology defines three types of bronchiectasis, according to the appearance of the affected bronchus, namely cylindrical, varicose and vesicular (or cystic).

See also Signet-ring sign.

Bronchiolectasis (bronquiolectasia)

Bronchiolectasis refers to the dilatation of a bronchiole. It is analogous to bronchiectasis, but it affects an airway of much smaller diameter, identified in the periphery of the lung (Figure 14). Bronchiolectasis manifests as rounded or tubular structures, generally located in the periphery of the lung, with thick walls or filled with secretion (see also Tree-in-bud pattern).^(3,7) It can also be combined with other pulmonary opacities and to the distortion of the parenchyma in cases of fibrosis.

See also Traction bronchiectasis and traction bronchiolectasis.

Traction bronchiectasis and traction bronchiolectasis (bronquiectasia e bronquiolectasia de tração)

Traction bronchiectasis and traction bronchiolectasis refer, respectively, to bronchial and bronchiolar dilatation secondary to the retraction of the parenchyma resulting from fibrosis

(Figure 13).⁽³⁾ They manifest as bronchial and bronchiolar dilatations, often irregular, associated with the distortion of the parenchyma due to fibrosis and other lung alterations (principally reticular opacities, ground-glass opacities and consolidations). They have a tubular, cystic or microcystic aspect (peripheral bronchioles), depending on the relationship between the bronchial axis or the bronchiolar axis and the CT scan slice. This last aspect can be confused with honeycombing, another alteration frequently associated with pulmonary fibrosis.⁽²⁸⁾

Cavitation (cavidade or escavação)

Cavities are gas-filled spaces, with or without air-fluid level, within a nodule, mass or pulmonary consolidation. They are typically produced by the expulsion or drainage of a necrotic part through the airway (Figure 15) or to the pleural space. The walls of a cavity are usually irregularly outlined and measure over 1 mm in thickness. The word “cavity” is not synonymous with “abscess”. Although the term “cavitation” can be translated to Portuguese as *cavitação* or *escavação*, the term *cavitação* has a different meaning in Portuguese and therefore should not be used as a synonym for *escavação* in this context.⁽⁷⁾

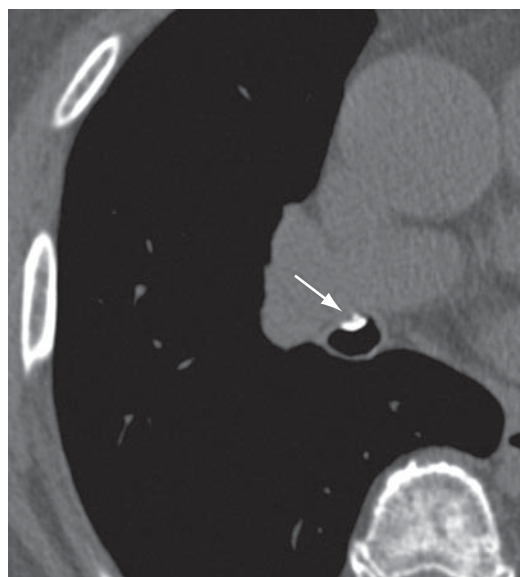


Figure 11 – Axial CT slice of the chest without the use of contrast material, revealing a broncholith (arrow).

Cyst (cisto)

A cyst is any rounded, well-circumscribed space surrounded by an epithelial or fibrous wall of variable thickness.⁽²⁹⁾ On CT scans, a cyst is

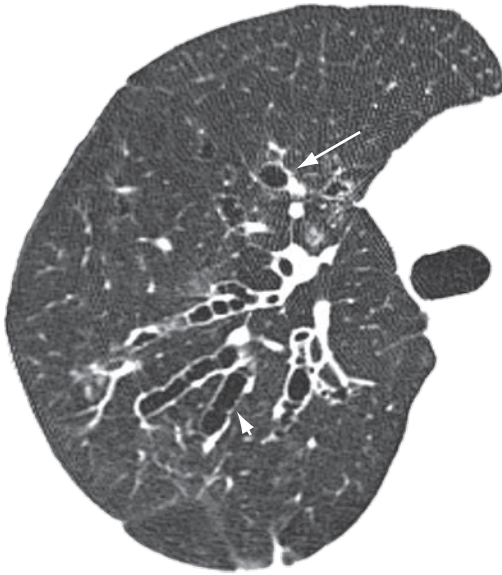


Figure 12 - Bronchiectasis characterized by the “signet-ring sign” (long arrow) and “tram tracks” appearance (short arrow).

seen as a rounded area with low attenuation coefficient on the lung parenchyma, having a well-defined interface with the adjacent normal lung (Figure 16).^(1,7) The cyst wall is usually thin (< 2 mm), but it can vary in thickness. Cysts are usually filled with air but can also contain liquid (e.g., bronchogenic cyst) or even a solid material. Diseases accompanied by multiple pulmonary cysts include lymphangiomyomatosis, Langerhans cell histiocytosis, lymphocytic interstitial pneumonia and Birt-Hogg-Dubé syndrome.^(30,31)

Collapse (colapso)

Collapse is generally used as a synonym for total atelectasis of one lobe or whole lung atelectasis (Figure 2).⁽⁷⁾

See also Atelectasis.

Consolidation (consolidação)

Consolidation is when the air in the alveolar spaces is supplanted by any type of pathological product, such as inflammatory exudate (pneumonia), transudate (edema), blood (alveolar hemorrhage), lipoprotein (alveolar proteinosis),

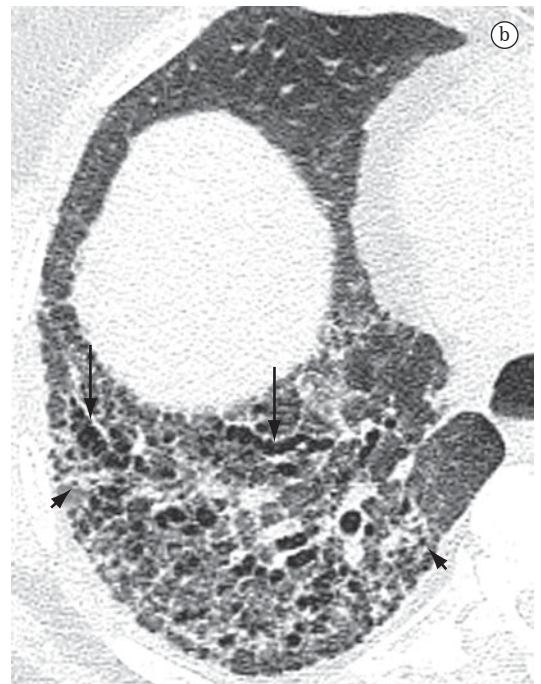
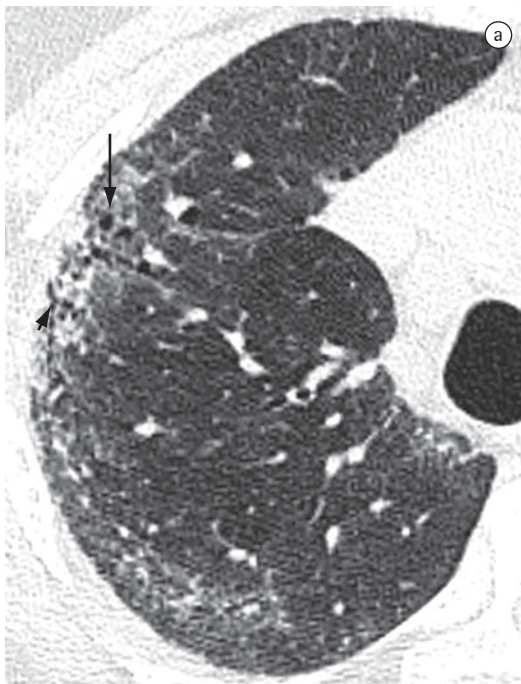


Figure 13 - Axial HRCT slices of the chest showing the right upper lobe (a) and the base of the right lung (b), revealing traction bronchiectasis (long arrows) and traction bronchiolectasis (short arrows) in a patient with interstitial fibrosis (nonspecific interstitial pneumonia), associated with distortion of the lung parenchyma and reticulate parenchyma, as well as with ground-glass opacities.

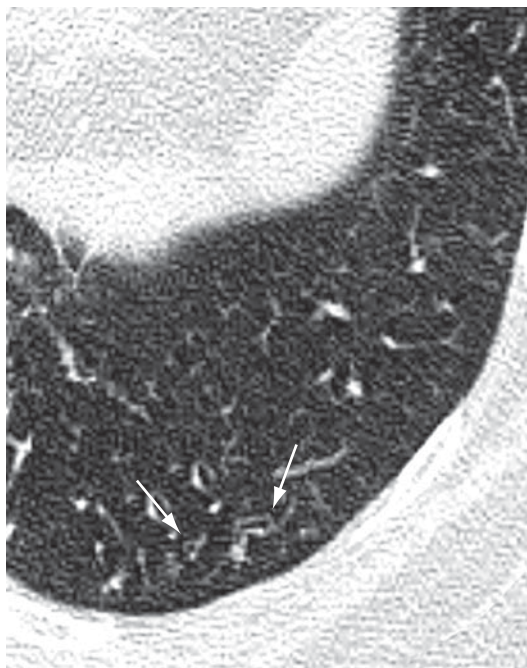


Figure 14 - Bronchiolectasis (arrows) located in the periphery of the lung.



Figure 15 - Cavity within an area of consolidation.

fat (lipoid pneumonia), cells (bronchioloalveolar carcinoma, lymphoma, organizing pneumonia) or gastric content (aspiration pneumonia).⁽³²⁾ On CT scans, it manifests as increased attenuation of the lung parenchyma, which hinders the visualization of the vessels and outer contours of the bronchial walls. Air bronchograms can be seen

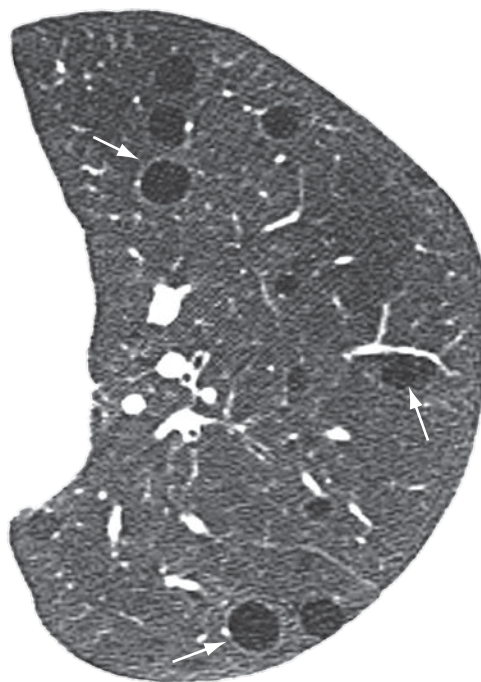


Figure 16 - Pulmonary cysts (arrows) in a patient with lymphangioleiomyomatosis.

(Figures 3 and 10). On CT scans, the attenuation value of the consolidated parenchyma without the use of contrast material is rarely useful for differential diagnosis, with the exception of specific situations (e.g., low attenuation in lipoid pneumonia and high attenuation in amiodarone toxicity).^(33,34)

Architectural distortion (distorção da arquitetura)

Architectural distortion is characterized by displacements in the path and/or distortions in the morphology of anatomical structures such as bronchi, vessels, fissures, or interlobular septa; it is usually related to caused by diffuse parenchymal diseases, particularly interstitial fibrosis.⁽⁷⁾ On HRCT scans, the loss of anatomical definition of the secondary lobule and the local volume reduction are considered signs of architectural distortion of the lobule and can be considered indirect signs of fibrosis (Figure 13).⁽³⁾

Pulmonary emphysema (enfisema pulmonar)

Pulmonary emphysema is characterized by permanently enlarged airspaces distal to the

terminal bronchiole with destruction of the alveolar walls.⁽³⁵⁾ The additional histological criterion of absence of “obvious fibrosis” has been questioned because some degree of interstitial fibrosis might be present due to smoking.⁽³⁶⁾ Emphysema is classified according to the acinar region affected: proximal (centriacinar or centrilobular emphysema), distal (paraseptal emphysema), or whole acinus (panacinar or panlobular emphysema).⁽³⁷⁾ The tomographic findings are areas of low attenuation, typically without visible walls.^(37,38)

Bullous emphysema (enfisema bolhoso)

Bullous emphysema is the bullous destruction of the parenchyma in combination with centriacinar emphysema, distal (paraseptal) emphysema or panacinar emphysema (Figure 17). It is designated giant bullous emphysema when the bullae, which might vary from 1 to over 20 cm in diameter, occupy at least one third of the hemithorax.^(7,39)

See also Bulla.

Centriacinar emphysema (enfisema centroacinar)

Centriacinar emphysema is the destruction of the walls of the centriacinar alveoli combined with an increase in respiratory bronchioles and associated alveoli. Centriacinar emphysema is the most common form of emphysema in cigarette smokers. Tomographic findings are centrilobular areas of decreased attenuation, usually without visible walls, having nonuniform distribution and predominantly located in the upper pulmonary regions (Figure 18).^(37,38) The centrilobular arteries can frequently be identified within the hypodense areas. The term centrilobular emphysema is commonly used as a synonym in CT.

Interstitial emphysema (enfisema intersticial)

Interstitial emphysema is characterized by the air dissection of the pulmonary interstitium, typically located on the bronchovascular sheaths, interlobular septa and visceral pleura; it is more frequently identified in neonates receiving mechanical ventilation (Figure 19). Interstitial emphysema is seldom recognized radiographically in adults and is rarely seen on CT scans. The process appears as areas of air density with

perivascular distribution, peribronchovascular distribution or distributed along the interlobular septa (Figure 20), or as rounded areas of low attenuation simulating small bullae or cysts (Figures 19 and 20).^(40,41)

Panacinar emphysema (enfisema panacinar)

Panacinar (panlobular) emphysema involves all portions of the acinus and, reasonably uniformly, the secondary pulmonary lobule.

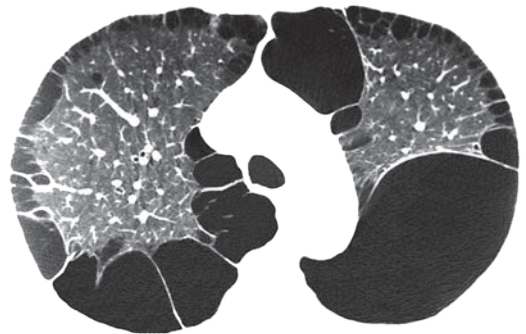


Figure 17 – Bilateral bullous emphysema.

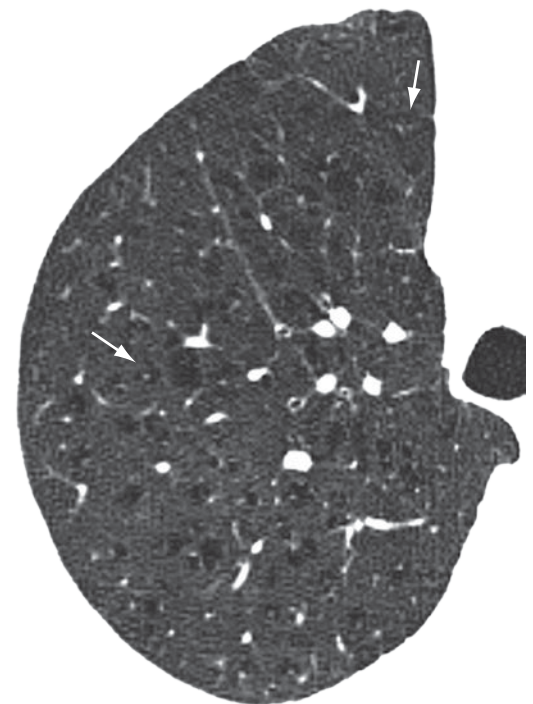


Figure 18 – Centriacinar (centrilobular) emphysema in the right upper lobe of a smoking patient. The centrilobular arteries (arrows) are identified within some areas of emphysema.

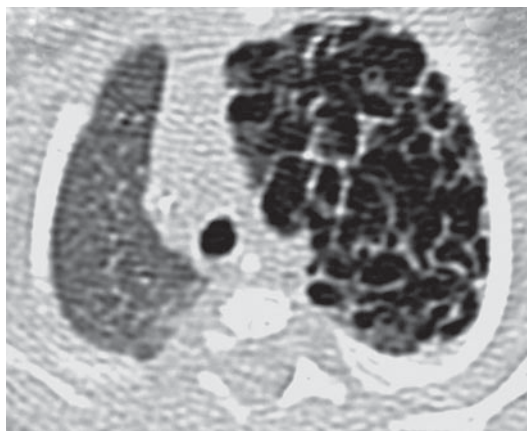


Figure 19 - Left diffuse interstitial emphysema in a neonatal patient.

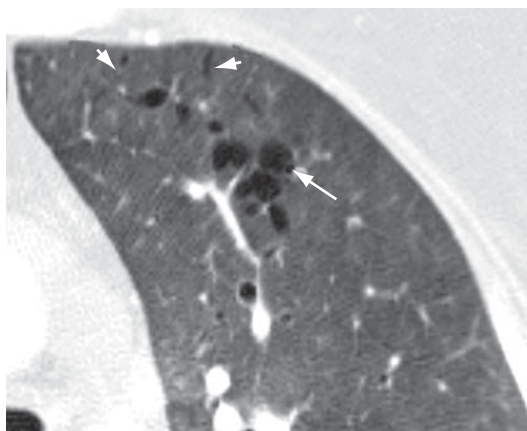


Figure 20 - Interstitial emphysema in an adult patient, characterized by rounded areas (arrow) and bands distributed along the interlobular septa (arrow heads) with air density.

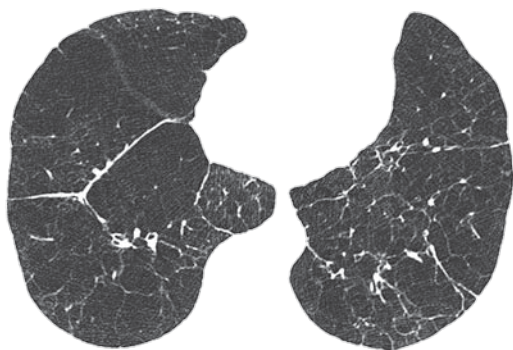


Figure 21 - Panacinar (panlobular) emphysema in the lower lobes of a patient with alpha-1 antitrypsin deficiency.

It predominates in the lower lobes and is the form of emphysema associated with alpha-1 antitrypsin deficiency. Panacinar emphysema is seen on CT scans as a generalized decrease in the attenuation of the lung with a reduction in the diameter of the blood vessels in the affected areas, with or without distortion of these vessels (Figure 21).^(37,38,42) Severe panacinar emphysema can coexist and merge with severe centriacinar emphysema. On CT scans, it can be indistinguishable from the findings of severe constrictive bronchiolitis.

Paraseptal, or distal acinar, emphysema (enfisema parasseptal/acinar distal)

Paraseptal emphysema affects predominantly the distal alveoli and their ducts and sacs. It is characteristically delimited by any pleural surface or interlobular septa. On CT scans, it is characterized by areas of low attenuation in the subpleural and peribronchovascular regions, separated by intact interlobular septum (Figure 22).^(37,38) It is sometimes associated with bullae.

Air spaces (espaços aéreos)

Air spaces correspond to the spaces bounded by the alveolar walls, including the alveolar sacs, alveolar ducts and the alveoli on the walls of the respiratory bronchioles.⁽⁴³⁾ This term can be used in association with consolidation, opacity or nodules to characterize the origin of such lesions, which fill these spaces with liquid or cells. The air bronchogram sign (Figures 3 and 10) is the trademark of air space filling.

See also Air bronchogram.

Interlobular septal thickening (essamento de septos interlobulares)

Interlobular septal thickening is the thickening of the connective tissue septa separating the secondary pulmonary lobules. It is radiographically characterized by thin linear opacities, also designated Kerley B lines. It is usually in close contact with the lateral pleural surface, near the costophrenic sulci, at a right angle to the pleural wall. Currently, the terms “septal lines” or “septal thickening” have gained favor over Kerley lines. On HRCT scans (Figure 23), the thickening of the interlobular septa is characterized by the presence of linear opacities that

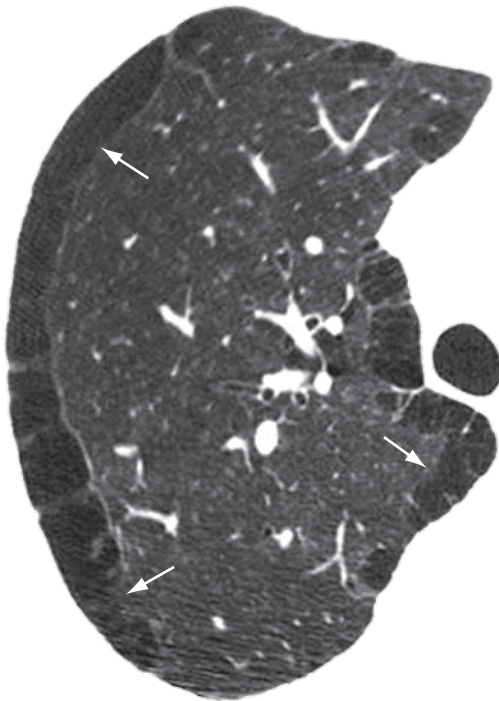


Figure 22 - Paraseptal, or distal acinar, emphysema in the right upper lobe (arrows).

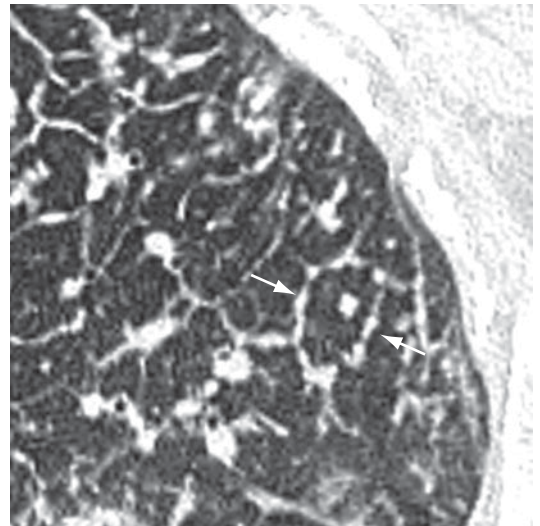


Figure 24 - Interlobular septal thickening of the nodular type (arrows), with a beaded appearance (beaded septum sign).

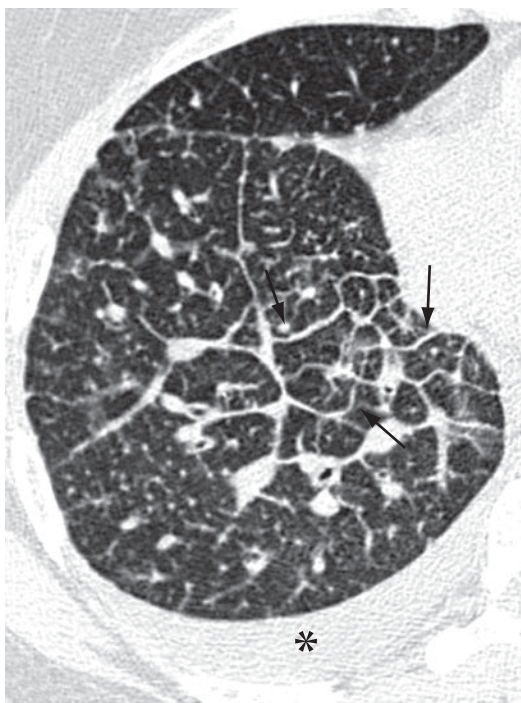


Figure 23 - Interlobular septal thickening (arrows) of the smooth type in a patient with pulmonary edema. Pleural effusion (asterisk).

delimit the secondary pulmonary lobules, more easily characterized in the subpleural region, in which it has the aspect of lines at right angles to the pleural surface.^(3,44) In the central regions of the lungs, the thickening of the septa of adjacent lobules results in the aspect of polygonal arches. Septal thickening can be secondary to changes in any of its components (veins, lymphatic vessels or connective tissue) and is a finding common to various lung alterations; however, its presence is particularly highlighted in cases of pulmonary edema and lymphangitic carcinomatosis. Septal thickening can be smooth (Figure 23), nodular (Figure 24) or irregular. This differentiation can aid in the differential diagnosis.

***Centrilobular region
(estruturas centrolobulares)***

The centrilobular region comprises the central portion of the secondary pulmonary lobule, consisting of the pulmonary artery, bronchiole and surrounding lung interstitium.⁽⁴⁵⁾ On HRCT scans of normal patients, it corresponds to a small nodular or linear image, located 3-10 mm from the pleural surface or the interlobular septum, representing the intralobular pulmonary artery and measuring approximately 1 mm in diameter (Figure 25).^(46,47) The corresponding bronchiole, when normal, has walls with approximate thickness of 0.15 mm, below the resolution limits of the HRCT. Therefore, the bronchiolar disease

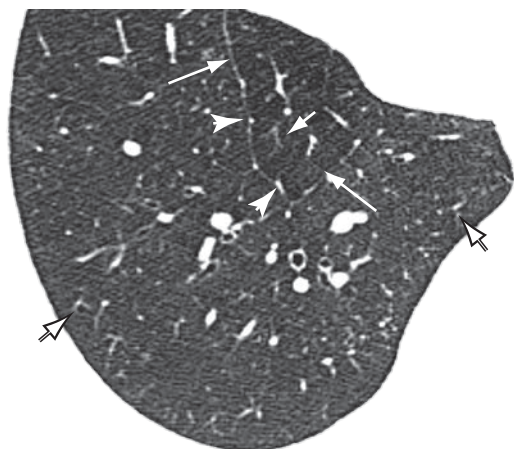


Figure 25 - Axial HRCT scan of the chest in a normal patient, revealing interlobular septa (long arrow) delineating the pulmonary lobule and centrilobular structures corresponding to the intralobular arteries, identified as small branched or nodular structures in the center of the pulmonary lobule. These are better seen on the HRCT scan in the periphery of the parenchyma (short arrow). The pulmonary veins (arrow heads) are seen within the interlobular septa.

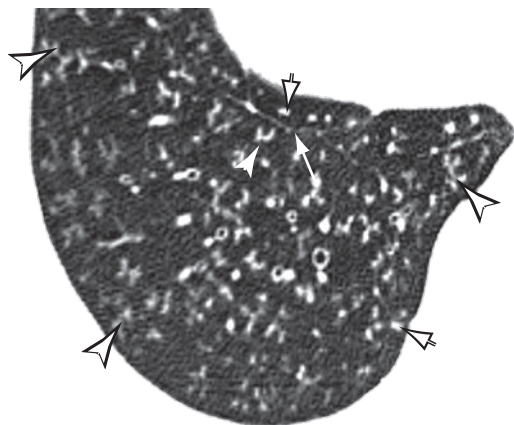


Figure 26 - Axial HRCT scan of the chest in a patient with small-airways disease (infectious bronchiolitis), revealing branching opacities (tree-in-bud pattern, indicated by the arrow heads) and small centrilobular nodules (short arrows). Some normal interlobular septa can be seen (long arrow).

that produces an enhancement of the centrilobular structure occurs when there is thickening of the bronchiolar wall or filling of the bronchiolar lumen (Figure 26). Centrilobular patterns include: (a) nodules; (b) tree-in-bud pattern; (c) thickening of the peribronchovascular peripheral interstitium; and (d) areas of low attenuation without visible walls (emphysema).

Honeycombing, or honeycomb lung (faveolamento, or favo de mel)

Honeycombing is characterized by pulmonary cysts created as a result of the destruction of the distal air spaces due to parenchymal fibrosis, with loss of acinar and bronchiolar architecture. Honeycombing cysts are covered with metaplastic bronchiolar epithelium and represent the end stage of a number of pulmonary diseases.^(1,48) On HRCT scans, honeycombing is characterized by multiple cysts, generally subpleural and of comparable diameters (typically 0.3-1 cm), grouped on layers and sharing well-defined walls of 1-3 mm in thickness (Figure 27).⁽⁴⁹⁾ Honeycombing is a tomographic marker of pulmonary fibrosis. The principal causes of honeycombing include idiopathic pulmonary fibrosis, collagenoses, chronic hypersensitivity pneumonitis, drug-induced pulmonary reactions and asbestosis.⁽²⁸⁾ It should be differentiated from paraseptal emphysema and traction bronchiolectasis.

Progressive massive fibrosis (fibrose maciça progressiva)

Progressive massive fibrosis is the conglomeration of small pulmonary nodules, generally accompanied by fibrosis (Figure 28). It is frequently bilateral and predominates in the upper lobes. It can be accompanied by an irregular increase in the size of the air space periphery. Progressive massive fibrosis is generally found in patients with a history of heavy exposure to inorganic dust (e.g., coal worker's pneumoconiosis and silicosis).⁽⁵⁰⁾ The tomographic findings of progressive massive fibrosis can be similar to those of sarcoidosis and talcosis.⁽⁵¹⁾

Fissure (fissura or cissura)

Fissure is the invagination of the visceral pleura that covers the outer surface of the lung to the parenchyma.⁽⁷⁾ Each interlobar fissure is formed by the juxtaposition of two layers of visceral pleura. In general, we can identify major (oblique) fissures, which separate the lower lobes from the others, and the lesser (horizontal) fissure, distinguishing the middle lobe from the right upper lobe (Figure 29). Supernumerary fissures are frequently found.

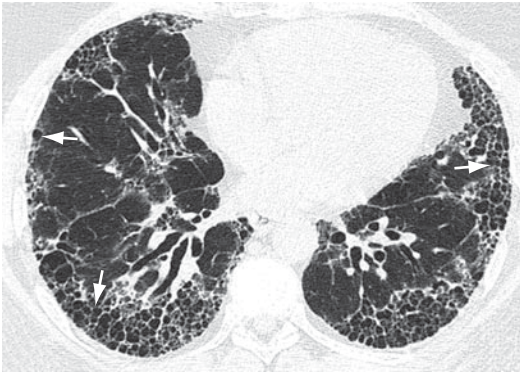


Figure 27 – Honeycombing cysts (arrows) in a patient with pulmonary fibrosis.

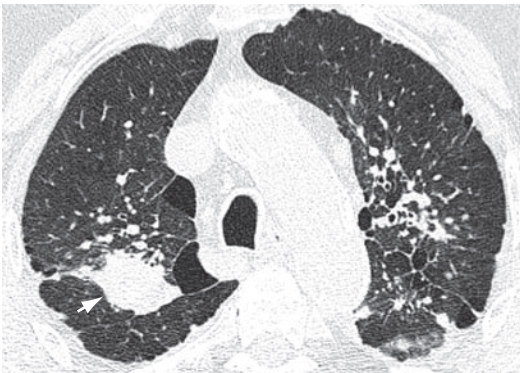


Figure 28 – Progressive massive fibrosis (arrow) in a patient with coal worker's pneumoconiosis.

Interface (interface)

An interface is the separation between two structures or spaces. When two thoracic structures with different radiological densities are juxtaposed, their boundaries are clear. For example, vessels presenting soft tissue density coming into contact with the air density of the surrounding ventilated lung. The “sign of the interface” defines the irregularity of the margins of different intrathoracic structures, such as vessels, bronchi and pleural surfaces, generally resulting from interstitial disease that causes fibrosis (Figure 30).⁽³⁾

Interstitialium (interstício)

The interstitium is a net of connective tissue that spreads over the lungs and is subdivided into: (a) axial (bronchovascular) interstitium—surrounding the bronchi, arteries and veins from the hila to the level of the respiratory bronchioles; (b) peripheral interstitium—composed

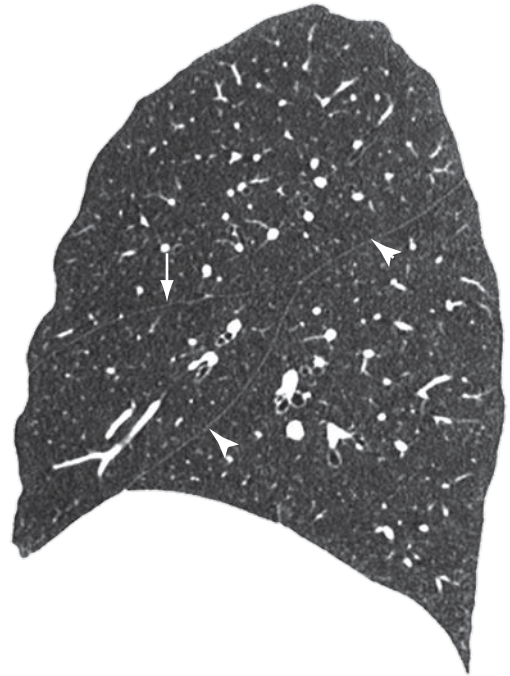


Figure 29 – Sagittal reformatting of the HRCT scan of the chest revealing a lesser fissure (arrow) and a major fissure (arrow heads) in the right lung.

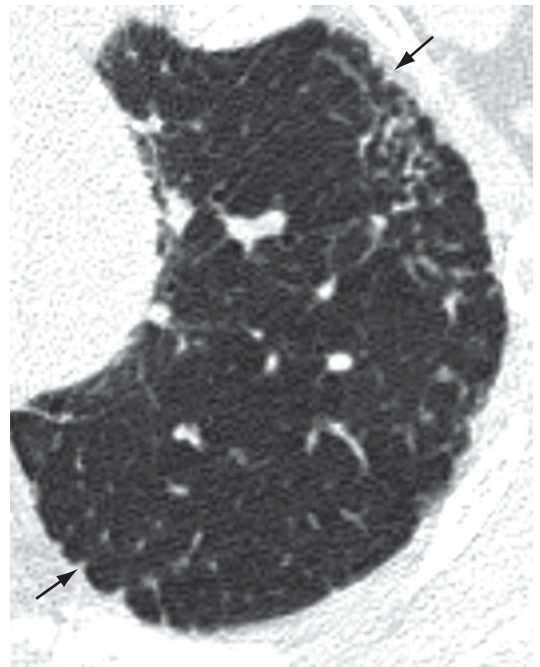


Figure 30 – Sign of the interface (arrows) in a patient with pulmonary fibrosis.

of the connective tissue contiguous to the pleural (subpleural) surfaces and interlobular septa; and (c) intralobular interstitium (also designated acinar or parenchymal interstitium)—composed of the alveolar walls (alveolar septa), and supporting the structure of the secondary pulmonary lobule.^(2,3,7)

Lymph node enlargement (linfonodomegalia)

Lymph node enlargement is characterized by the increase in volume in one or more lymph nodes, due to any cause, surpassing the dimensional limits considered normal for the lymph node chain in question (Figure 31).^(52,53) The term “adenomegaly” is not an acceptable synonym, since lymph nodes are not true glandular structures. The term “*linfonodopatia*” (“lymphatic disease”) is reserved for situations in which a disease, such as necrosis, has been identified within a lymph node.

Subpleural curvilinear line (linha curvilínea subpleural)

The subpleural curvilinear line is a curvilinear opacity of 1–3 mm in thickness, located in the subpleural region and having a parallel distribution over the pleural surface (Figure 32). It is a nonspecific sign for atelectasis, edema, fibrosis or inflammation.^(3,7)

Intralobular lines (linhas intralobulares)

Intralobular lines are seen on HRCT scans as thin linear images within the secondary pulmonary lobule. When numerous, they can have a fine reticular aspect (Figure 33). This finding can be seen in different conditions, especially in cases of fibroses (e.g., usual interstitial pneumonia) and diseases associated with the crazy-paving pattern (e.g., alveolar proteinosis).^(3,54)

See also Reticular pattern and Crazy-paving pattern.

Secondary pulmonary lobule (lóbulo pulmonar secundário)

The secondary pulmonary lobule is the smallest anatomic unit of lung delimited by a septum of connective tissue. It is polyhedral in shape, measures 1.0–2.5 cm in diameter and contains a variable number of acini.⁽⁴⁵⁾ The

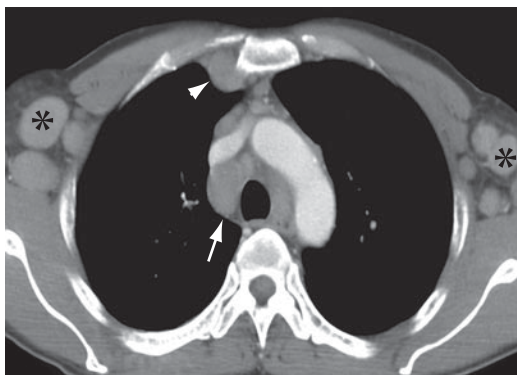


Figure 31 – Axial CT slice of the chest with iodinated contrast material revealing enlarged mediastinal lymph nodes (arrow), chest wall lymph node enlargement (arrow head) and bilateral axillary lymph node enlargement (asterisks).



Figure 32 – Bilateral curvilinear lines (arrows).



Figure 33 – Intralobular lines (arrows) associated with ground-glass opacities.

center of the lobule is formed by the bronchiole and its accompanying pulmonary artery, lymphatic vessels and adjacent interstitium. In its periphery, the connective tissue forms thin septa designated interlobular septa, which contain small pulmonary veins and lymphatic vessels (Figure 25). In normal patients, the interlobular septa are better identified in the anterior, lateral and paramediastinal peripheral regions of the upper and middle lobes, as well as in the peripheral region of the anterior diaphragmatic region of the lower lobes, tending to be incomplete or absent in the remaining lung regions. The interlobular septa are easily recognized on HRCT scans when the septal interstitium is affected (Figures 23 and 24).⁽³⁾

Mass (*massa*)

A mass is any expansive pulmonary, pleural, mediastinal or chest wall lesion presenting

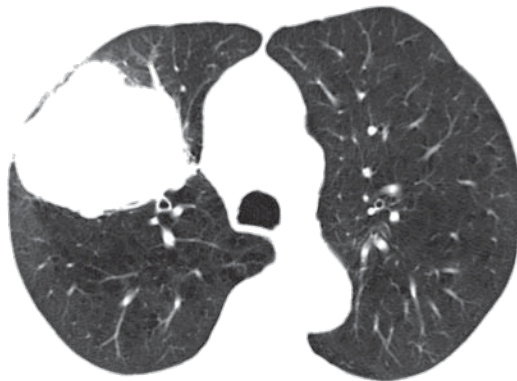


Figure 34 - Pulmonary mass in the right upper lobe measuring 5.5 cm in diameter.

density of soft, fatty or bony tissue; greater than 3 cm in diameter; with at least partially defined contours; outside of the topography of the fissures and independent of the characteristics of its contours or the heterogeneity of its content (Figure 34).⁽⁷⁾

Mycetoma (micetoma)

A mycetoma characteristically represents a group of subcutaneous chronic infections caused by the traumatic inoculation into the skin of material contaminated with actinomycetes, principally *Nocardia brasiliensis*, or eumycetes, resulting in actinomycetoma and eumycetoma, respectively.⁽²⁰⁾ It tends to invade adjacent tissues, forming nodules or masses with cavities and fistulous pathways, with the elimination of suppurative secretion containing grains constituted by masses of hyphae and filaments. In most cases, it is located in the lower limbs and can cause deformities and fractures. Pulmonary and pleural involvement is rare.⁽⁵⁵⁾ When the lung is affected, the aspect is of consolidation with necrosis, and pleural effusion can be seen.⁽⁵⁶⁾ Mycetoma generally affects agriculturists and is endemic in Latin America, India and Africa.^(20,57) Mycetoma is not a colonization of a preexisting pulmonary cavity; therefore, the use of this term as a synonym for “fungus ball” should be avoided.

See also Fungus ball.

Nodule (nódulo)

A nodule is a focal opacity that is rounded, or at least partially delineated, smaller than 3.0



Figure 35 - Axial HRCT slices of the chest in three patients revealing pulmonary nodules (arrows) with different attenuation: a) solid (soft tissue density); b) non-solid (ground-glass attenuation); and c) part-solid or semisolid.

cm in diameter and generally presenting soft tissue or calcified tissue density (Figure 35). When the opacity is smaller than 10 mm, it is recommended that the term “small nodule” be used. When the opacity is smaller than 3 mm, it is recommended that the term “micronodule” be used.^(3,7) Nodules should be described according to the characteristics of their borders (well- or ill-defined), to their location or to their distribution (random, perilymphatic, centrilobular or pleural). With regard to attenuation, nodules can be classified as solid (Figure 35a), when they completely obscure the parenchyma; as non-solid (ground-glass attenuation), when they do not obscure the vascular margins and bronchial walls (Figure 35b); or as part-solid or semisolid (ground-glass opacity with solid areas), when they partially obscure the vascular margins and the bronchial walls (Figure 35c).⁽⁷⁾

See also Mass.

Oligemia (oligoemia)

Oligemia is a focal, regional or generalized reduction in pulmonary blood volume. It appears as a decrease in the diameter and number of pulmonary vessels (regional or wide-spread), indicating less than normal blood flow (Figure 36).^(3,7)

Opacity (opacidade)

Opacity is an image which, due to its greater density, is at least partially distinguishable from the surrounding or superimposed structures. On chest X-rays, this term does not specify the pathological nature, size or specific location of the image. An opacity can be caused by an abnormality in the lung, pleura or chest wall, as well as by an external object. On CT scans, the pulmonary opacities can represent ground-glass opacity or consolidation.

See also Consolidation.

Ground-glass opacity/attenuation (opacidade/atenuação em vidro fosco)

On CT scans, ground-glass opacity corresponds to increased density of the lung parenchyma in which it is still possible to identify the contours of the vessels and bronchi within the area affected by a pathological process (Figure 37). This image pattern is related to interstitial thickening, partial filling of air spaces,

partial collapse of alveoli, increased capillary blood volume or a combination of all of these mechanisms.^(58,59) Ground-glass attenuation should be distinguished from “consolidation” (Figures 10 and 38), in which the vessels are not identifiable within the affected area of the lung.

See also Consolidation.

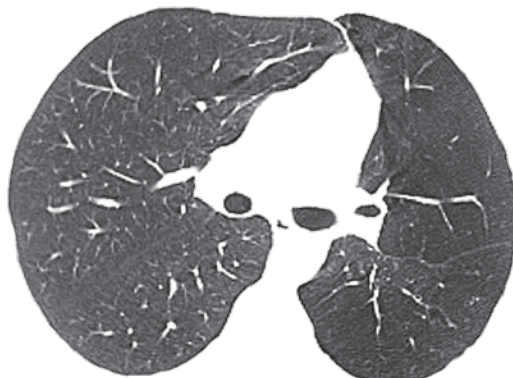


Figure 36 – Oligemia affecting the left lung.

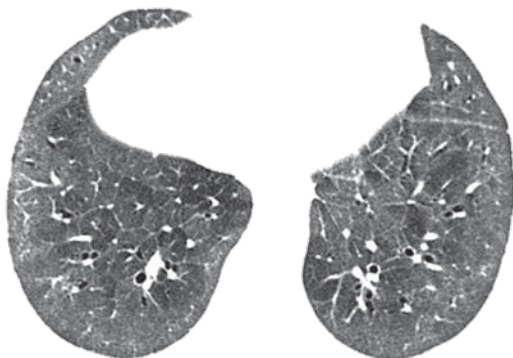


Figure 37 – Diffuse ground-glass opacity/attenuation in patient with progressive systemic sclerosis.

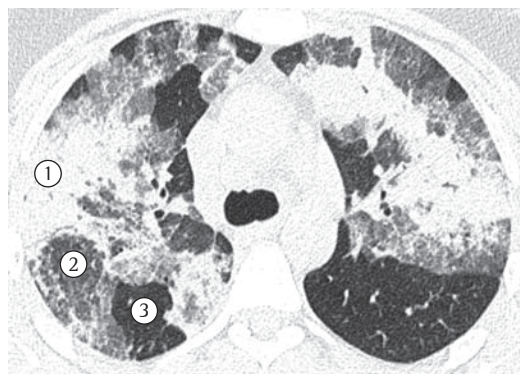


Figure 38 – Increased attenuation in the lung parenchyma (parenchymal opacification), characterized by areas of consolidation (1) and ground-glass opacities (2). In 3, lung with normal attenuation.

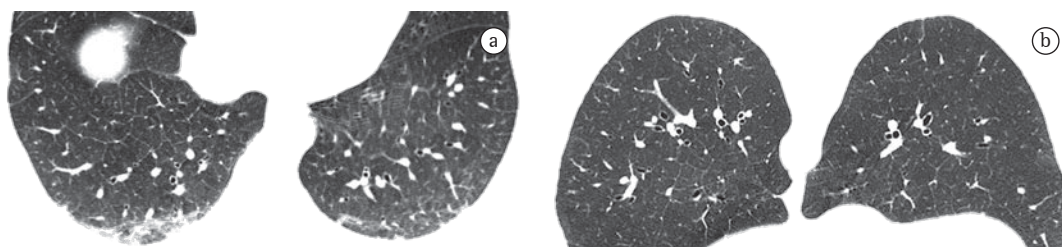


Figure 39 – Axial HRCT slice of the chest with the patient in the supine position. Hanging opacities in posterior subpleural regions of the lung (a) disappear when the patient is no longer horizontal (b).

Linear opacity (opacidade linear)

Linear opacity is characterized by a thin, elongated linear image with soft tissue density. Rarely, calcification or foreign material, which can increase the attenuation, is seen. It is a nonspecific term used for a number of etiologies. It is recommended that more specific terms be used whenever possible, such as “laminar atelectasis”, “parenchymal band” and “interlobular septal thickening”.

Hanging opacity (opacidade pendente)

A hanging opacity is defined as a subpleural opacity in one of the “hanging pulmonary regions”, which are areas of atelectasis that appear when the patient is lying down. Hanging opacities are seen in posterior regions when the patient is in the supine position (Figure 39a) and in anterior regions when the patient is in the prone position. They disappear when the patient is no longer in a horizontal position (Figure 39b).⁽⁴⁾

Parenchymal opacification (opacidade/opacificação parenquimatosa)

Parenchymal opacification is the increased attenuation in the lung parenchyma that can potentially obscure the contours of the vessels and bronchi. The term “consolidation” indicates that the margins of these structures are not visible (except for air bronchograms), and “ground-glass attenuation” indicates that, despite the altered lung density, the vessels and airways remain identifiable.^(4,32) It is recommended that the more specific terms “consolidation” and “ground-glass opacity” be used (Figure 38).

Tree-in-bud pattern (padrão de árvore em brotamento)

The tree-in-bud pattern represents centrilobular branching opacities with small nodules at the extremities that resembling the budding of certain trees (Figure 26).^(3,45) In most cases, this pattern represents dilated bronchioles filled with pathological material, although it might also be associated with infiltration of the peribronchial connective tissue in the centrilobular vasculature or, occasionally, with dilatation or filling (e.g., intravascular metastases) of the centrilobular arteries.^(60,61) This finding is often indicative of disease affecting the airways and is particularly common in infectious processes (e.g., tuberculosis, bronchopneumonia and infectious bronchiolitis) but it can also be found in a number of other diseases (e.g., bronchiectasis, cystic fibrosis and panbronchiolitis).⁽⁴⁷⁾

Mosaic attenuation/perfusion pattern (padrão de atenuação/perfusão em mosaico)

The mosaic attenuation pattern appears as patchwork of regions of differing attenuation that can represent infiltrative lung disease, obliterative small-airways disease or occlusive vascular disease (Figure 40).^(62,63) Air trapping secondary to bronchial or bronchiolar obstruction can produce parenchymal foci of lower attenuation, which become more evident in expiratory CT scans.⁽⁸⁾ In obliterative small-airways disease and vascular occlusive disease, the areas of low attenuation are abnormal; in general, the number and size of pulmonary vessels in these areas are reduced when compared with those in the adjacent normal lung, which might present normal or increased attenuation (due to redirec-

tion of blood flow). Mosaic attenuation pattern can also be caused by parenchymal pulmonary disease, characterized by ground-glass opacity; in this case, the areas with increased attenua-

tion are the affected regions and the remaining regions characterize foci of preserved lung.^(3,7)

See also Air trapping.

Crazy-paving pattern (padrão de pavimentação em mosaico)

The crazy-paving pattern presents superimposition of ground-glass opacities, interlobular lines and thickened interlobular septa (Figure 41). The interface between the normal and the affected lungs tends to be well-delimited in this pattern of pulmonary lesion. This pattern was initially identified in patients with pulmonary alveolar proteinosis, but it can also be seen in other diffuse pulmonary diseases in which the interstitial and alveolar compartments are affected (e.g., pulmonary hemorrhage).^(1,2,64)

Centrilobular nodules (padrão nodular centrolobular)

Centrilobular nodules are small nodules located in the center of the secondary pulmonary lobule, generally related to bronchiolar diseases, pulmonary artery diseases or peribronchovascular bundle diseases.⁽⁷⁾ The principal tomographic finding is that these nodules are located at a distance of a few millimeters from the pleural surface and the fissures (Figure 42a).⁽⁴⁵⁻⁴⁷⁾ The most common cause of this condition is inhalation-related diseases (e.g., hypersensitivity pneumonitis, silicosis and respiratory bronchiolitis). If it is accompanied by the tree-in-bud pattern (Figure 26), infectious causes should be considered (e.g., tuberculosis and bronchopneumonia).

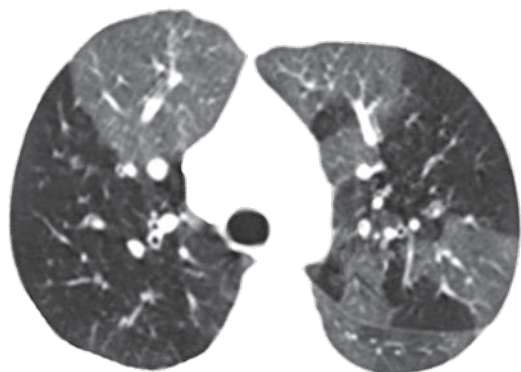


Figure 40 - Bilateral mosaic attenuation pattern, caused by obliterative small-airways disease.



Figure 41 - Crazy-paving pattern.

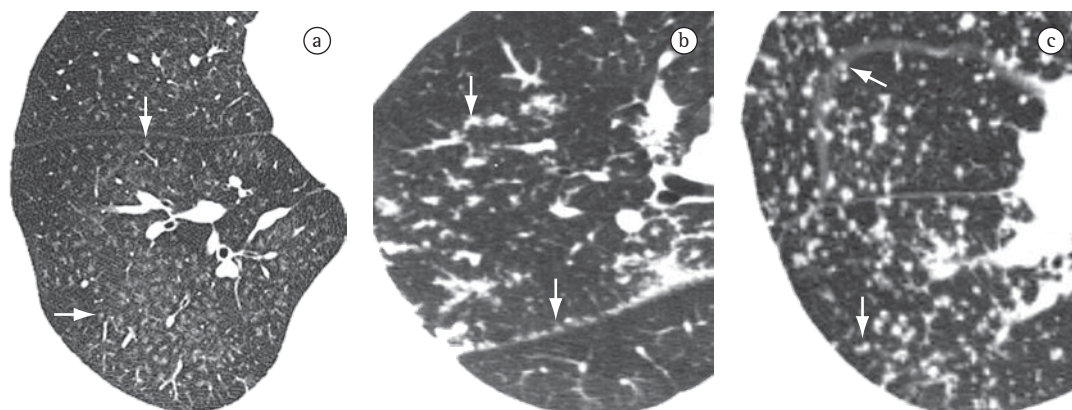


Figure 42 - Small nodules (arrows) with centrilobular (a), perilymphatic (b) and random (c) distribution.

***Perilymphatic nodules
(padrão nodular perilinfático)***

The perilymphatic nodular pattern is characterized by a pattern of distribution of small nodules along the pulmonary lymphatic system (interlobular septa, peribronchovascular bundle and pleural surface) (Figure 42b). The principal diseases accompanied by perilymphatic nodules are sarcoidosis and lymphangitic carcinomatosis.^(45,65)

Miliary nodules—See Random, or miliary, nodules

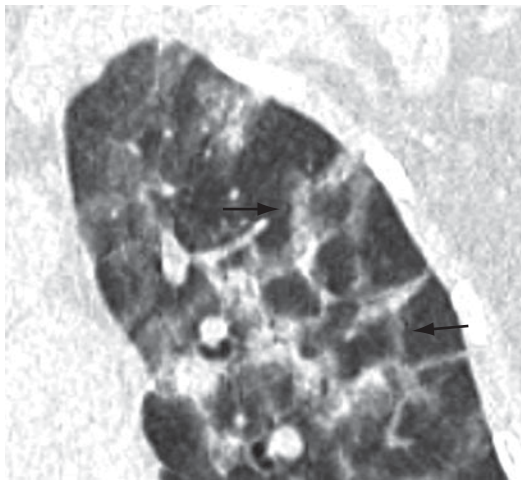


Figure 43 – Perilobular pattern (arrows).

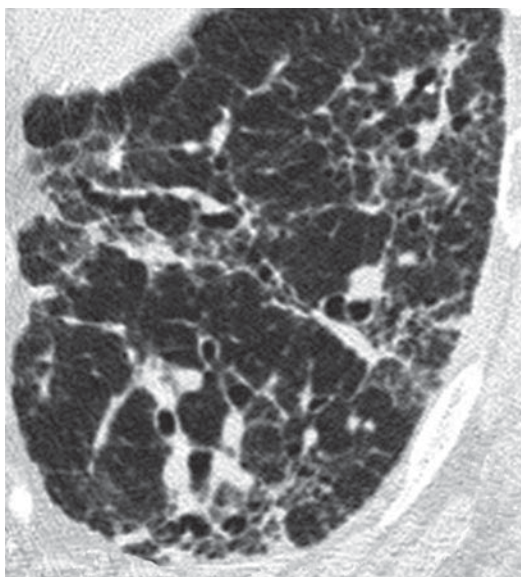


Figure 44 – Reticular pattern in a patient with pulmonary fibrosis.

***Random, or miliary, nodules
(padrão nodular randômico, or miliar)***

The random distribution of small nodules throughout the lungs (Figure 42c) is most often caused by miliary tuberculosis, miliary histoplasmosis or hematogenous metastases.^(3,45,65)

Perilobular pattern (padrão perilobular)

The perilobular pattern is characterized by the distribution of abnormality along the structures that border the pulmonary lobules, that is, the interlobular septa, the visceral pleura and major pulmonary vessels.⁽⁶⁶⁾ The term is more frequently used in the context of diseases (e.g., perilobular organizing pneumonia) that are distributed principally around the periphery of the secondary lobule. On CT scans, it is characterized by the presence of thick and irregular polygonal opacities in the periphery of the secondary pulmonary lobule (Figure 43).⁽⁶⁷⁾ It should be distinguished from the interlobular septal thickening (septal pattern), because it is thicker and more irregular; and from the reversed halo sign.

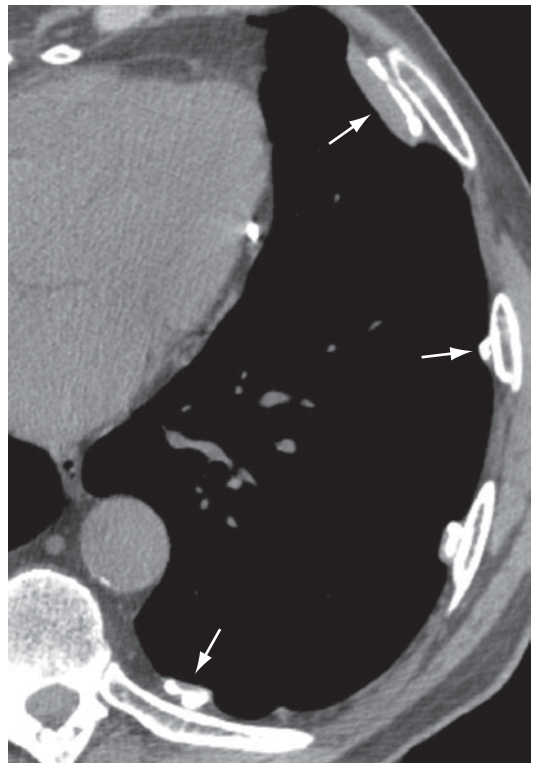


Figure 45 – Pleural plaques with calcification (arrows) in a patient exposed to asbestos.

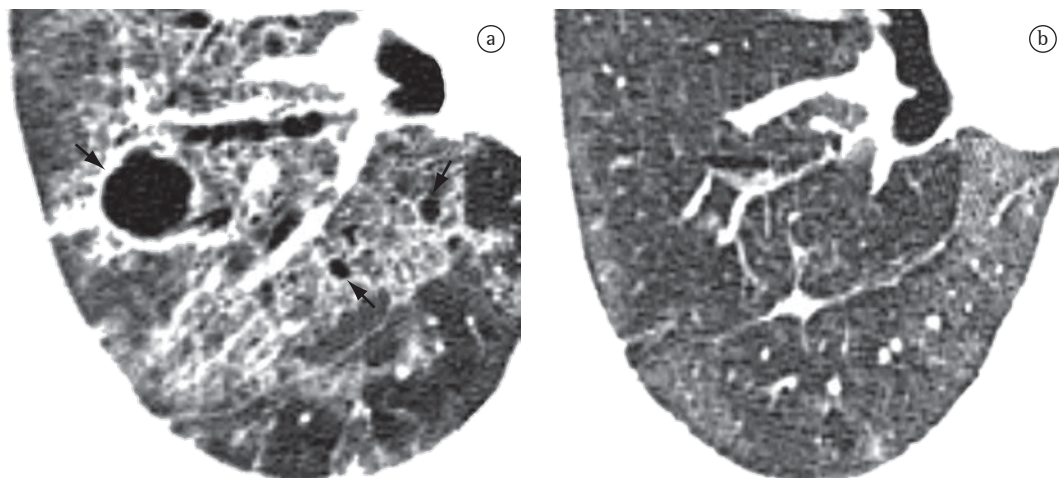


Figure 46 - Axial CT slice of the chest. In a, pneumatocele (arrows) and ground-glass opacities in patient with pneumonia by *Pneumocystis jirovecii*. In b, HRCT scan obtained after two months, showing diminution in the areas of ground-glass opacity and resolution of the pneumatocele.

See also Septal pattern and Reversed halo sign.

Reticular pattern (padrão reticular)

The reticular pattern is an alteration that is usually associated with interstitial diseases and is radiographically characterized by innumerable linear opacities that produce a net-like appearance.⁽¹⁾ On HRCT scans, it is possible to single out the components responsible for this radiographic pattern, usually related to the presence of interlobular and septal lines (Figure 44) or to the presence of cysts with walls giving the radiographic appearance of lines, such as in pulmonary cystic diseases, in bullae-related emphysema and even in honeycombing cysts.^(1,3,7)

See also Intralobular lines.

Pleural plaque (placa pleural)

Pleural plaque is focal pleural thickening, occasionally presenting calcification, of variable thickness and up to 5 cm in extension (Figure 45).⁽⁶⁸⁾ It usually occurs in the subcostal parietal pleural surface or diaphragm pleura. When the plaques are multiple and bilateral, they are almost always caused by exposure to asbestos.^(69,70)

Pneumatocele (pneumatocele)

Pneumatocele is a gas-filled space with walls formed by distended air spaces. It changes in size frequently over a short period of time because

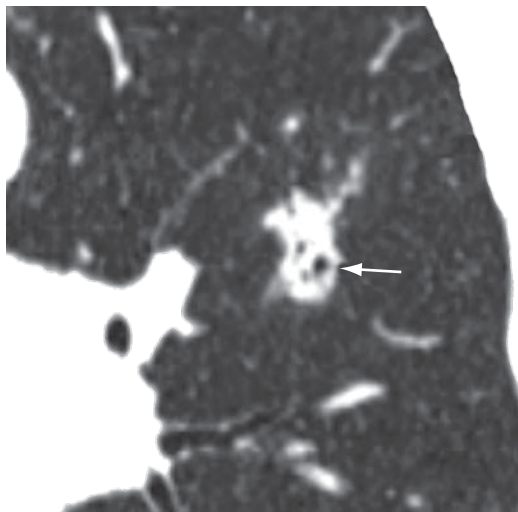


Figure 47 - Pseudocavities (arrow) in a patient with adenocarcinoma.

of its characteristic mechanism of check-valve airway obstruction.⁽⁷¹⁾ Pneumatocele is usually associated with infectious diseases, especially those caused by *Staphylococcus* sp. in children and *Pneumocystis* sp. in adults. On CT scans, it manifests as a rounded air space bounded by thin walls, within the lung (Figure 46a).^(3,7) It can resolve spontaneously, even if tardily, while the infection is being treated (Figure 46b).

Pseudocavity (pseudocavidade)

A pseudocavity is a round or oval-shaped area of low attenuation in nodules, pulmo-

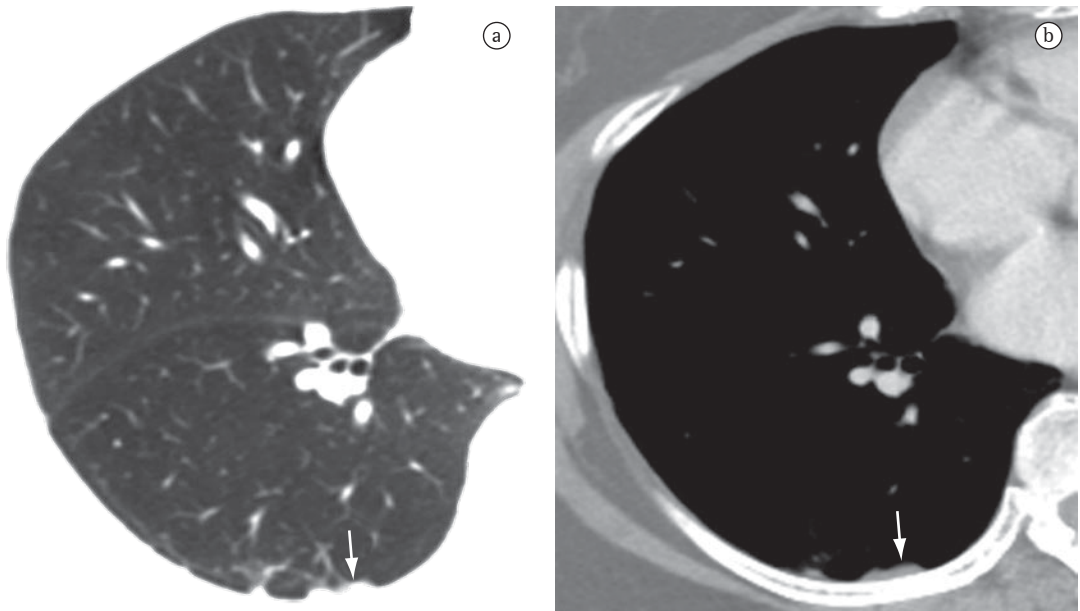


Figure 48 – Axial CT slices of the chest with iodinated contrast material reconstructed using algorithms for the evaluation of the lung parenchyma (A) and mediastinum (B), revealing pseudoplaque (arrows).

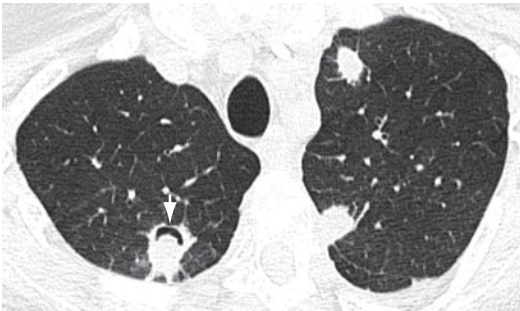


Figure 49 – Nodule showing the air crescent sign (arrow) in a patient with bilateral angioinvasive aspergillosis.

nary masses or areas of consolidation within a portion of preserved pulmonary parenchyma, within dilated or normal bronchi or (as an area of emphysema) within a lesion (Figure 47). Pseudocavities generally measure less than 1 cm in diameter. They can be seen in patients with adenocarcinoma, bronchioloalveolar carcinoma or pneumonia.^(7,72)

Pseudoplaque (pseudoplaça)

A pseudoplaque is a peripheral pulmonary opacity, adjacent to the visceral pleura and formed by small, coalescent pulmonary nodules that simulate the pleural plaque (Figure 48).⁽⁷³⁾ It

is more commonly found in sarcoidosis, silicosis and coal workers' pneumoconiosis.

Signet-ring sign (sinal do anel de sinete)

The signet-ring sign is a sign composed of a ring-like opacity representing a dilated bronchus, together with a smaller, rounded opacity contiguous to the bronchial wall, representing its artery (pulmonary artery or, rarely, the bronchial artery), resembling a “signet ring” or a “pearl ring”.⁽⁷⁴⁾ It is the basic tomographic sign of bronchiectasis (Figure 12).^(26,75) Occasionally, the signet-ring sign can also be found in diseases characterized by an abnormal reduction in pulmonary arterial flow, such as chronic pulmonary thromboembolism and proximal interruption of the pulmonary artery.⁽⁷⁶⁾

See also Bronchiectasis.

Air crescent sign (sinal do crescente aéreo)

The air crescent sign corresponds to a collection of air of variable size and in the form of a crescent or half moon, located in the periphery of a nodule or mass and presenting soft tissue density; in the proper clinical context, this finding is suggestive of angioinvasive aspergil-

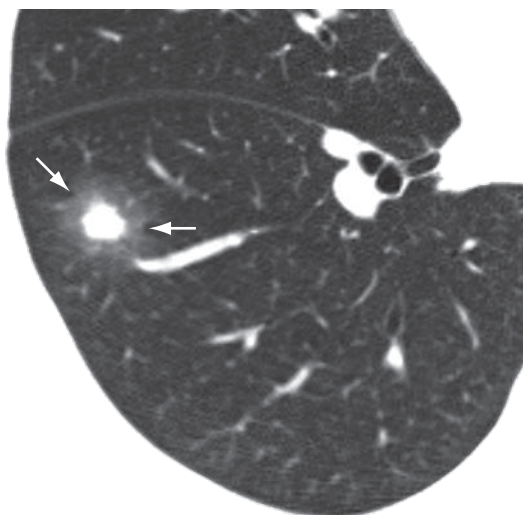


Figure 50 - Nodule showing the halo sign (arrows).

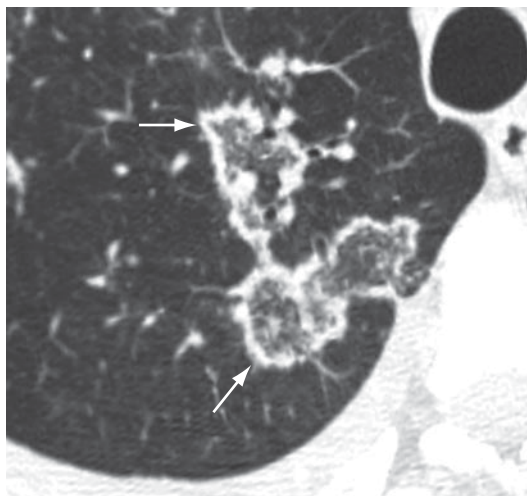


Figure 51 - Reversed halo sign (arrows).

losis in the recovery phase (Figure 49).⁽⁷⁷⁻⁷⁹⁾ In this case, the air crescent sign is secondary to the retraction of infarcted pulmonary parenchyma and the resorption of necrotic tissue in the peripheral region of the lesion, causing the space between the dead tissue and the adjacent parenchyma to be filled by air.⁽⁷⁸⁾ This sign is also used to describe the findings of the fungus ball, in which there is a collection of air surrounding the intracavitary lesion or interposed between the upper wall of the preexisting cavity and the hanging intracavitary lesion (Figure 7).⁽⁷⁾ The air crescent sign has also been described in other diseases, such as intracavitary hemorrhage, bacterial abscess and lung cancer.^(80,81)

See also Fungus ball.

Halo sign (sinal do halo)

The halo sign is characterized by a ground-glass opacity surrounding a nodule, mass or round area of consolidation (Figure 50). It was initially described as a sign of hemorrhage surrounding a focus of angioinvasive aspergillosis.⁽⁸²⁾ The halo sign appears early and is highly specific to neutropenic patients with fever.⁽⁸²⁾ It can be caused by hemorrhage associated with other types of disease (e.g., candidiasis and Kaposi's sarcoma) or by local pulmonary infiltration by neoplasm (e.g., adenocarcinoma).⁽⁸³⁻⁸⁶⁾

Reversed halo sign (sinal do halo invertido)

The reversed halo sign is a ground-glass opacity surrounded by a complete or partially complete ring of consolidation (Figure 51). Although it was initially described as a sign of organizing pneumonia, it has also been associated with other diseases, such as paracoccidioidomycosis.^(87,88)

Beaded septum sign (sinal do septo nodular em contas/rosário)

The beaded septum sign is an irregular and nodular thickening of the interlobular septa resembling a row of beads (Figure 24).⁽⁷⁾ Although it was initially described as a sign of lymphangitic carcinomatosis, it is more frequently found in sarcoidosis.⁽⁸⁹⁾

Acknowledgments

Our special thanks to Dr. Jorge Issamu Kavakama, a brilliant radiologist who has influenced generations with his talent, charisma and enthusiasm and was an active participant in the development and publication of the previous versions of the Brazilian Consensus on the terms used for chest CT findings.

References

1. Müller NL, Silva CI. Interstitial patterns. In: Müller NL, Silva CI, editors. *Imaging of the Chest*. Philadelphia: Saunders; 2008. p. 158-99.
2. Webb RW, Müller NL, Naidich DP. High-resolution computed tomography findings of lung disease. In: Webb RW, Müller NL, Naidich DP, editors. *High-resolution CT*

- of the lung. 4th ed. Philadelphia: Lippincott Williams & Wilkins; 2009. p. 65-176.
3. Webb RW, Müller NL, Naidich DP. Illustrated glossary of high-resolution computed tomography terms. In: Webb WR, Muller NL, Naidich DP, editors. High-resolution CT of the lung. Philadelphia: Lippincott Williams & Wilkins; 2009. p. 585-602.
 4. Austin JH, Müller NL, Friedman PJ, Hansell DM, Naidich DP, Remy-Jardin M, et al. Glossary of terms for CT of the lungs: recommendations of the Nomenclature Committee of the Fleischner Society. *Radiology*. 1996;200(2):327-31.
 5. Departamento de Imagem da Sociedade Brasileira de Pneumologia e Tisiologia. Brazilian Consensus on Terminology Used in order to Describe Computed Tomography of the Chest. *J Bras Pneumol*. 2005;31(2):149-56.
 6. Souza Jr AS, Araujo NT, Jasinovodolinski D, Marchiori E, Kavakama J, Irion KL, et al. Terminologia para a descrição de tomografia computadorizada do tórax: sugestões iniciais para um consenso brasileiro. *Radiol Bras*. 2002;35(2):125-28.
 7. Hansell DM, Bankier AA, MacMahon H, McLoud TC, Müller NL, Remy J. Fleischner Society: glossary of terms for thoracic imaging. *Radiology*. 2008;246(3):697-722.
 8. Arakawa H, Webb WR, McCowin M, Katsou G, Lee KN, Seitz RF. Inhomogeneous lung attenuation at thin-section CT: diagnostic value of expiratory scans. *Radiology*. 1998;206(1):89-94.
 9. Webb WR. High-resolution computed tomography of obstructive lung disease. *Radiol Clin North Am*. 1994;32(4):745-57.
 10. Arakawa H, Webb WR. Air trapping on expiratory high-resolution CT scans in the absence of inspiratory scan abnormalities: correlation with pulmonary function tests and differential diagnosis. *AJR Am J Roentgenol*. 1998;170(5):1349-53.
 11. Tuddenham WJ. Glossary of terms for thoracic radiology: recommendations of the Nomenclature Committee of the Fleischner Society. *AJR Am J Roentgenol*. 1984;143(3):509-17.
 12. Molina PL, Hiken JN, Glazer HS. Imaging evaluation of obstructive atelectasis. *J Thorac Imaging*. 1996;11(3):176-86.
 13. Woodring JH, Reed JC. Types and mechanisms of pulmonary atelectasis. *J Thorac Imaging*. 1996;11(2):92-108.
 14. Westcott JL, Cole S. Plate atelectasis. *Radiology*. 1985;155(1):1-9.
 15. Cohen AM, Crass JR, Chung-Park M, Tomaszewski JF Jr. Rounded atelectasis and fibrotic pleural disease: the pathologic continuum. *J Thorac Imaging*. 1993;8(4):309-12.
 16. McHugh K, Blaquiére RM. CT features of rounded atelectasis. *AJR Am J Roentgenol*. 1989;153(2):257-60.
 17. O'Donovan PB, Schenk M, Lim K, Obuchowski N, Stoller JK. Evaluation of the reliability of computed tomographic criteria used in the diagnosis of round atelectasis. *J Thorac Imaging*. 1997;12(1):54-8.
 18. Akira M, Yamamoto S, Yokoyama K, Kita N, Morinaga K, Higashihara T, Kozuka T. Asbestosis: high-resolution CT-pathologic correlation. *Radiology*. 1990;176(2):389-94.
 19. Roberts CM, Citron KM, Strickland B. Intrathoracic aspergilloma: role of CT in diagnosis and treatment. *Radiology*. 1987;165(1):123-8.
 20. Ameen M, Arenas R. Developments in the management of mycetomas. *Clin Exp Dermatol*. 2009;34(1):1-7.
 21. Martinez S, Heyneman LE, McAdams HP, Rossi SE, Restrepo CS, Eraso A. Mucoïd impactions: finger-in-glove sign and other CT and radiographic features. *Radiographics*. 2008;28(5):1369-82.
 22. Collins J. CT signs and patterns of lung disease. *Radiol Clin North Am*. 2001;39(6):1115-35.
 23. Reed JC, Madewell JE. The air bronchogram in interstitial disease of the lungs. A radiological-pathological correlation. *Radiology*. 1975;116(1):1-9.
 24. Conces DJ Jr, Tarver RD, Vix VA. Broncholithiasis: CT features in 15 patients. *AJR Am J Roentgenol*. 1991;157(2):249-53.
 25. Seo JB, Song KS, Lee JS, Goo JM, Kim HY, Song JW, et al. Broncholithiasis: review of the causes with radiologic-pathologic correlation. *Radiographics*. 2002;22:S199-213.
 26. Naidich DP, McCauley DI, Khouri NF, Stitik FP, Siegelman SS. Computed tomography of bronchiectasis. *J Comput Assist Tomogr*. 1982;6(3):437-44.
 27. Grenier P, Maurice F, Musset D, Menu Y, Nahum H. Bronchiectasis: assessment by thin-section CT. *Radiology*. 1986;161(1):95-9.
 28. Lynch DA, Travis WD, Müller NL, Galvin JR, Hansell DM, Grenier PA, et al. Idiopathic interstitial pneumonias: CT features. *Radiology*. 2005;236(1):10-21.
 29. Genereux GP. The end-stage lung: pathogenesis, pathology, and radiology. *Radiology*. 1975;116(02):279-89.
 30. Hartman TE. CT of cystic diseases of the lung. *Radiol Clin North Am*. 2001;39(6):1231-44.
 31. Grant LA, Babar J, Griffin N. Cysts, cavities, and honeycombing in multisystem disorders: differential diagnosis and findings on thin-section CT. *Clin Radiol*. 2009;64(4):439-48.
 32. Leung AN, Miller RR, Müller NL. Parenchymal opacification in chronic infiltrative lung diseases: CT-pathologic correlation. *Radiology*. 1993;188(1):209-14.
 33. Laurent F, Philippe JC, Vergier B, Granger-Veron B, Darpeix B, Vergeret J, et al. Exogenous lipid pneumonia: HRCT, MR, and pathologic findings. *Eur Radiol*. 1999;9(6):1190-6.
 34. Kuhlman JE, Scatarige JC, Fishman EK, Zerhouni EA, Siegelman SS. CT demonstration of high attenuation pleural-parenchymal lesions due to amiodarone therapy. *J Comput Assist Tomogr*. 1987;11(1):160-2.
 35. Thurlbeck WM, Müller NL. Emphysema: definition, imaging, and quantification. *AJR Am J Roentgenol*. 1994;163(5):1017-25.
 36. Cardoso WV, Sekhon HS, Hyde DM, Thurlbeck WM. Collagen and elastin in human pulmonary emphysema. *Am Rev Respir Dis*. 1993;147(4):975-81.
 37. Takahashi M, Fukuoka J, Nitta N, Takazakura R, Nagatani Y, Murakami Y, et al. Imaging of pulmonary emphysema: a pictorial review. *Int J Chron Obstruct Pulmon Dis*. 2008;3(2):193-204.
 38. Foster WL Jr, Gimenez EI, Roubidoux MA, Sherrier RH, Shannon RH, Roggli VL, et al. The emphysemas: radiologic-pathologic correlations. *Radiographics*. 1993;13(2):311-28.

39. Stern EJ, Webb WR, Weinacker A, Müller NL. Idiopathic giant bullous emphysema (vanishing lung syndrome): imaging findings in nine patients. *AJR Am J Roentgenol.* 1994;162(2):279-82.
40. Kemper AC, Steinberg KP, Stern EJ. Pulmonary interstitial emphysema: CT findings. *AJR Am J Roentgenol.* 1999;172(6):1642.
41. Donnelly LF, Lucaya J, Ozelame V, Frush DP, Strouse PJ, Sumner TE, et al. CT findings and temporal course of persistent pulmonary interstitial emphysema in neonates: a multiinstitutional study. *AJR Am J Roentgenol.* 2003;180(4):1129-33.
42. Spouge D, Mayo JR, Cardoso W, Müller NL. Panacinar emphysema: CT and pathologic findings. *J Comput Assist Tomogr.* 1993;17(5):710-3.
43. Murata K, Khan A, Herman PG. Pulmonary parenchymal disease: evaluation with high-resolution CT. *Radiology.* 1989;170(3 Pt 1):629-35.
44. Kang EY, Grenier P, Laurent F, Müller NL. Interlobular septal thickening: patterns at high-resolution computed tomography. *J Thorac Imaging.* 1996;11(4):260-4.
45. Webb WR. Thin-section CT of the secondary pulmonary lobule: anatomy and the image--the 2004 Fleischner lecture. *Radiology.* 2006;239(2):322-38.
46. Gruden JF, Webb WR, Warnock M. Centrilobular opacities in the lung on high-resolution CT: diagnostic considerations and pathologic correlation. *AJR Am J Roentgenol.* 1994;162(3):569-74.
47. Murata K, Itoh H, Todo G, Kanaoka M, Noma S, Itoh T, et al. Centrilobular lesions of the lung: demonstration by high-resolution CT and pathologic correlation. *Radiology.* 1986;161(3):641-5.
48. Genereux GP. The end-stage lung: pathogenesis, pathology, and radiology. *Radiology.* 1975;116(02):279-89.
49. Primack SL, Hartman TE, Hansell DM, Müller NL. End-stage lung disease: CT findings in 61 patients. *Radiology.* 1993;189(3):681-6.
50. Chong S, Lee KS, Chung MJ, Han J, Kwon OJ, Kim TS. Pneumoconiosis: comparison of imaging and pathologic findings. *Radiographics.* 2006;26(1):59-77.
51. Ward S, Heyneman LE, Reittner P, Kazerooni EA, Godwin JD, Müller NL. Talcosis associated with IV abuse of oral medications: CT findings. *AJR Am J Roentgenol.* 2000;174(3):789-93.
52. Glazer GM, Gross BH, Quint LE, Francis IR, Bookstein FL, Orringer MB. Normal mediastinal lymph nodes: number and size according to American Thoracic Society mapping. *AJR Am J Roentgenol.* 1985;144(2):261-5.
53. Mountain CF, Dresler CM. Regional lymph node classification for lung cancer staging. *Chest.* 1997;111(6):1718-23.
54. Webb WR, Stein MG, Finkbeiner WE, Im JG, Lynch D, Gamsu G. Normal and diseased isolated lungs: high-resolution CT. *Radiology.* 1988;166(1 Pt 1):81-7.
55. Abd El-Bagi ME, Fahal AH. Mycetoma revisited. Incidence of various radiographic signs. *Saudi Med J.* 2009;30(4):529-33.
56. Muñoz-Hernández B, Noyola MC, Palma-Cortés G, Rosete DP, Galván MA, Manjarrez ME. Actinomycetoma in arm disseminated to lung with grains of *Nocardia brasiliensis* with peripheral filaments. *Mycopathologia.* 2009;168(1):37-40.
57. Lacaz CS. Distribuição geográfica dos micetomas no Brasil. *An Bras Dermatol.* 1981;56(3):167-72.
58. Remy-Jardin M, Remy J, Giraud F, Watinne L, Gosselin B. Computed tomography assessment of ground-glass opacity: semiology and significance. *J Thorac Imaging.* 1993;8(4):249-64.
59. Remy-Jardin M, Giraud F, Remy J, Copin MC, Gosselin B, Duhamel A. Importance of ground-glass attenuation in chronic diffuse infiltrative lung disease: pathologic-CT correlation. *Radiology.* 1993;189(3):693-8.
60. Aquino SL, Gamsu G, Webb WR, Kee ST. Tree-in-bud pattern: frequency and significance on thin section CT. *J Comput Assist Tomogr.* 1996;20(4):594-9.
61. Franquet T, Giménez A, Prats R, Rodríguez-Arias JM, Rodríguez C. Thrombotic microangiopathy of pulmonary tumors: a vascular cause of tree-in-bud pattern on CT. *AJR Am J Roentgenol.* 2002;179(4):897-9.
62. Worthy SA, Müller NL, Hartman TE, Swensen SJ, Padley SP, Hansell DM. Mosaic attenuation pattern on thin-section CT scans of the lung: differentiation among infiltrative lung, airway, and vascular diseases as a cause. *Radiology.* 1997;205(2):465-70.
63. Martin KW, Sagel SS, Siegel BA. Mosaic oligemia simulating pulmonary infiltrates on CT. *AJR Am J Roentgenol.* 1986;147(4):670-73.
64. Rossi SE, Erasmus JJ, Volpacchio M, Franquet T, Castiglioni T, McAdams HP. "Crazy-paving" pattern at thin-section CT of the lungs: radiologic-pathologic overview. *Radiographics.* 2003;23(6):1509-19.
65. Colby TV, Swensen SJ. Anatomic distribution and histopathologic patterns in diffuse lung disease: correlation with HRCT. *J Thorac Imaging.* 1996;11(1):1-26.
66. Johkoh T, Müller NL, Ichikado K, Nakamura H, Itoh H, Nagareda T. Perilobular pulmonary opacities: high-resolution CT findings and pathologic correlation. *J Thorac Imaging.* 1999;14(3):172-7.
67. Ujita M, Renzoni EA, Veeraraghavan S, Wells AU, Hansell DM. Organizing pneumonia: perilobular pattern at thin-section CT. *Radiology.* 2004;232(3):757-61.
68. Lynch DA, Gamsu G, Aberle DR. Conventional and high resolution computed tomography in the diagnosis of asbestos-related diseases. *Radiographics.* 1989;9(3):523-51.
69. Friedman AC, Fiel SB, Fisher MS, Radecki PD, Lev-Toaff AS, Caroline DF. Asbestos-related pleural disease and asbestosis: a comparison of CT and chest radiography. *AJR Am J Roentgenol.* 1988;150(2):269-75.
70. Aberle DR, Gamsu G, Ray CS, Feuerstein IM. Asbestos-related pleural and parenchymal fibrosis: detection with high-resolution CT. *Radiology.* 1988;166(3):729-34.
71. Quigley MJ, Fraser RS. Pulmonary pneumatocele: pathology and pathogenesis. *AJR Am J Roentgenol.* 1988;150(6):1275-7.
72. Weisbrod GL, Chamberlain D, Herman SJ. Cystic change (pseudocavitation) associated with bronchioloalveolar carcinoma: a report of four patients. *J Thorac Imaging.* 1995;10(2):106-11.
73. Remy-Jardin M, Beuscart R, Sault MC, Marquette CH, Remy J. Subpleural micronodules in diffuse infiltrative lung diseases: evaluation with thin-section CT scans. *Radiology.* 1990;177(1):133-9.
74. Ouellette H. The signet ring sign. *Radiology.* 1999;212(1):67-8.
75. McGuinness G, Naidich DP, Leitman BS, McCauley DI. Bronchiectasis: CT evaluation. *AJR Am J Roentgenol.* 1993;160(2):253-9.

76. Remy-Jardin M, Remy J, Louveigny S, Artaud D, Deschildre F, Duhamel A. Airway changes in chronic pulmonary embolism: CT findings in 33 patients. *Radiology*. 1997;203(2):355-60.
77. Curtis AM, Smith GJ, Ravin CE. Air crescent sign of invasive aspergillosis. *Radiology*. 1979;133(1):17-21.
78. Kuhlman JE, Fishman EK, Burch PA, Karp JE, Zerhouni EA, Siegelman SS. CT of invasive pulmonary aspergillosis. *AJR Am J Roentgenol*. 1988;150(5):1015-20.
79. Abramson S. The air crescent sign. *Radiology*. 2001;218(1):230-2.
80. Marshall GB, Farnquist BA, MacGregor JH, Burrowes PW. Signs in thoracic imaging. *J Thorac Imaging*. 2006;21(1):76-90.
81. Wang LF, Chu H, Chen YM, Perng RP. Adenocarcinoma of the lung presenting as a mycetoma with an air crescent sign. *Chest*. 2007;131(4):1239-42.
82. Kuhlman JE, Fishman EK, Siegelman SS. Invasive pulmonary aspergillosis in acute leukemia: characteristic findings on CT, the CT halo sign, and the role of CT in early diagnosis. *Radiology*. 1985;157(3):611-4.
83. Primack SL, Hartman TE, Lee KS, Müller NL. Pulmonary nodules and the CT halo sign. *Radiology*. 1994;190(2):513-5.
84. Gaeta M, Blandino A, Scribano E, Minutoli F, Volta S, Pandolfo I. Computed tomography halo sign in pulmonary nodules: frequency and diagnostic value. *J Thorac Imaging*. 1999;14(2):109-13.
85. Kim Y, Lee KS, Jung KJ, Han J, Kim JS, Suh JS. Halo sign on high resolution CT: findings in spectrum of pulmonary diseases with pathologic correlation. *J Comput Assist Tomogr*. 1999;23(4):622-6.
86. Lee YR, Choi YW, Lee KJ, Jeon SC, Park CK, Heo JN. CT halo sign: the spectrum of pulmonary diseases. *Br J Radiol*. 2005;78(933):862-5.
87. Kim SJ, Lee KS, Ryu YH, Yoon YC, Choe KO, Kim TS, et al. Reversed halo sign on high-resolution CT of cryptogenic organizing pneumonia: diagnostic implications. *AJR Am J Roentgenol*. 2003;180(5):1251-4.
88. Gasparetto EL, Escuissato DL, Davaus T, de Cerqueira EM, Souza AS Jr, Marchiori E, et al. Reversed halo sign in pulmonary paracoccidioidomycosis. *AJR Am J Roentgenol*. 2005;184(6):1932-4.
89. Ren H, Hruban RH, Kuhlman JE, Fishman EK, Wheeler PS, Zerhouni EA, et al. Computed tomography of inflation-fixed lungs: the beaded septum sign of pulmonary metastases. *J Comput Assist Tomogr*. 1989;13(3):411-6.

About the authors

C Isabela S Silva

Associate Researcher. Department of Radiology, University of British Columbia, Vancouver, Canada.

Edson Marchiori

Full Professor. Radiology Department, Fluminense Federal University, Niterói, Brazil.

Arthur Soares Souza Júnior

Adjunct Professor. *Faculdade de Medicina de São José do Rio Preto* – FAMERP, São José do Rio Preto School of Medicine – São José do Rio Preto, Brazil.

Nestor L. Müller

Full Professor. Department of Radiology, University of British Columbia, Vancouver, Canada.

Comissão de Imagem da Sociedade Brasileira de Pneumologia e Tisiologia, Biênio 2008–2010

The members of the Committee were Alexandre Dias Mançano, Carmem Lúcia Fujita, Cesar Augusto de Araújo Neto, Dante L. Escuissato, Dany Jasinowodolinski, Gustavo de Souza Portes Meirelles, Jorge L. Pereira Silva, José Antônio Baddini Martinez, Klaus L. Irion, Luiz Felipe Nobre, Marcelo Buarque de Gusmão Funari, Marcelo Pereira Chaves, Mário Terra Filho and Pedro A. Daltró.